*accepted version: https://doi.org/10.1007/s00477-020-01926-6*

# A revised range of variability approach considering the morphological alteration of hydrological indicators

Xin Zheng[a,*], Tao Yang[a], Tong Cui[b], Chong-Yu Xu[c], Xudong Zhou[d], Zhenya Li[a] and Pengfei Shi[a], Youwei Qin[a]

[a] *State Key Laboratory of Hydrology-Water Resources and Hydraulic Engineering, Center for Global Change and Water Cycle, Hohai University, Nanjing 210098, China*

[b] *Department of Hydraulic Engineering, Tsinghua University, Beijing 100084, China*

[c] *Department of Geosciences, University of Oslo, Sem Saelands vei 1, P.O. Box 1047 Blindern, N-0316 Oslo, Norway*

[d] *Institute of industrial science, the University of Tokyo, Tokyo, Japan*

## Declarations

**Funding**

This research was funded by grants from the National Natural Science Foundation of China (51879068, 51809072), and Graduate research and innovation projects in Jiangsu Province (KYCX20_0463).

**Conflicts of interest/Competing interests**

None

**Availability of data and material**

The dataset is available at https://figshare.com/articles/rawdata_csv/10053290.

**Code availability**

Relevant software applications and custom codes that support the findings of this study are available from the corresponding author upon reasonable request.

**Authors' contributions**

All authors contributed to the study conception and design. Material preparation, data collection and analysis were performed by Xin Zheng, Chongyu Xu, Xudong Zhou, Pengfei Shi, Zhenya

[*] Corresponding author at: State Key Laboratory of Hydrology-Water Resources and Hydraulic Engineering, Hohai University, Nanjing 210098, China.

E-mail addresses: xzheng@hhu.edu.cn (Xin Zheng), tao.yang@hhu.edu.cn (Tao Yang)

*accepted version: https://doi.org/10.1007/s00477-020-01926-6*

Li, and Youwei Qin. The methodology was proposed by Xin Zheng, Tong Cui and Tao Yang. The first draft of the manuscript was written by Xin Zheng and all authors commented on previous versions of the manuscript. All authors read and approved the final manuscript.

*accepted version: https://doi.org/10.1007/s00477-020-01926-6*

**Abstract**

A reasonable assessment of the hydrological regime is a prerequisite for river utilization, restoration, and protection. Although the hydrological alteration has been quantified with different indicators (IHAs) and the most widely used assessment methods (Range of Variability Approach, RVA), the morphological characteristic which demonstrates the overall hydrological regime is neglected. This will lead to an incomplete assessment of the hydrological alteration. To supplement the current assessment, this work proposed a revised RVA method in three main steps: 1) to identify the morphological characteristics of each IHA; 2) to quantify the morphological alteration by comparing the Hasse matrices of different time series; 3) to combine the frequency alteration and morphological alteration of IHAs for reflecting overall hydrological alteration. A case study of the upper Yellow River shows that the revised RVA method outperforms RVA in the assessment of the hydrological regime not only because revised RVA captures the hydrological changes of certain IHAs that are not reflected by conventional RVA, but also the alteration identified by revised RVA shows more apparent differences at two stations upstream and downstream the dam than conventional RVA can provide. The revised RVA is more applicable to identify the hydrological alteration due to dam construction which could have negative impacts on river ecosystem since the morphological alteration of time series is considered. As a whole, the new method offers a better understanding of the alteration in hydrological regime, which gives beneficial guidance to river management.

**Keywords:** Time series analysis; Hydrological alteration; Yellow River; Range of variability approach (RVA)

*accepted version: https://doi.org/10.1007/s00477-020-01926-6*

## 1 Introduction

The hydrological regime, which shows the variations in the state and characteristics of the water body, is essential for maintaining a healthy river ecosystem [*Wang et al.*, 2016]. While strong alteration of hydrological regime due to human activities and climate change has led to serious problems on river ecosystem and neighboring inhabitants in many rivers over globe [*Zhang et al.*, 2016; *Tonkin et al.*, 2018]. In this case, proper assessments for the alteration can help better understand how the hydrological regime is changing and how the changes extract impacts on the ecosystem [*Suen et al.*, 2006].

The analyzing method Range of Variability Approach (RVA) combined with the Indicators of Hydrological Alteration (IHAs) has been proven successful and powerful in the assessment of hydrological regime alteration [*Richter et al.*, 1997, 1998; *Zolezzi et al.*, 2009; *Chen et al.*, 2010; *Eum et al.*, 2017]. IHAs contains a total number of 32 indices, which can be categorized into five groups based on their ecological implications (Table 1) [*Richter et al.*, 1996; *Cui et al.*, 2018]. RVA evaluates the alteration of hydrological regime by comparing IHAs derived from discharge series in pre-impact and post-impact periods, respectively. The IHA estimated in each year is divided into three ranges by two user-defined quantiles (e.g., 33% and 67% or 25% and 75%), which is named as RVA boundaries. The number of years when the IHA falling into the two RVA boundaries is counted and the frequency difference in two defined periods thus represents the degree of hydrological alteration. RVA has been extensively used in practice due to its simplicity and capability in many kinds of studies. *Yang et al.* (2008) applied RVA to evaluate the spatial alteration of the hydrological regime caused by large dam construction in the Yellow River basin. *Suen et al.* (2010) analyzed the relationship between climate change and hydrological regime alteration in Taiwan.

*accepted version: https://doi.org/10.1007/s00477-020-01926-6*

Table 1. Description of 32 IHAs

| IHA parameters group | Regime characteristics | Hydrologic parameters |
|---|---|---|
| Group 1: Magnitude of monthly water conditions | Magnitude<br>Timing | Mean value for each calendar month |
| Group 2: Magnitude and duration of annual extreme water conditions | Magnitude<br>Duration | 1-day minimum<br>3-day minimum<br>7-day minimum<br>30-day minimum<br>90-day minimum<br>1-day maximum<br>3-day maximum<br>7-day maximum<br>30-day maximum<br>90-day maximum<br>Base-flow index |
| Group 3: Timing of annual extreme water conditions | Timing | Julian date of each annual 1- day minimum<br>Julian date of each annual 1- day maximum |
| Group 4: Frequency and duration of high and low pulses | Magnitude<br>Frequency<br>Duration | Number of low pulses each year<br>Mean or median duration of low pulses<br>Number of high pulses each year<br>Mean or median duration of high pulses |
| Group 5: Rate and frequency of water condition changes | Frequency<br>Rate of change | Rise rate<br>Fall rate<br>Number of reversals |

However, RVA does not fully assess the hydrological alteration because only the occurrence changes in the middle range are considered to represent the hydrological regimes [*Huang et al.*, 2017]. Here we verify this argument by a set of real discharge data (Figure 1). The monthly streamflow of September, one of IHAs, has changed a lot since 1989 as the mean discharge and temporal variation has decreased. Moreover, the occurrence of high-flows events decreased in the following 20 years. However, the frequency of this IHA values falling into the middle range was not changed compared to pre-impacted period. Thus, RVA fails to detect the changes in this specific indicator. To settle the problem, many studies focused on revising this method [*Lin et al.*, 2016; *Yu et al.*, 2016; *McDaniel et al.*, 2019]. *Shiau and Wu* [2008] developed a histogram matching approach to consider the variations of IHA values within and out of the statistical range. *Yang et al.* [2014] thought that human activities might also change the periodicity of streamflow and proposed a revised RVA to reflect the periodicity alteration of IHAs. *Yin et al.* [2015] used the Euclidean distance rather than a single indicator to measure the alterations between the hydrologic years. *Ge et al.* [2018] combined a first-order connectivity index with RVA results to distinguish the influence of different indicators.

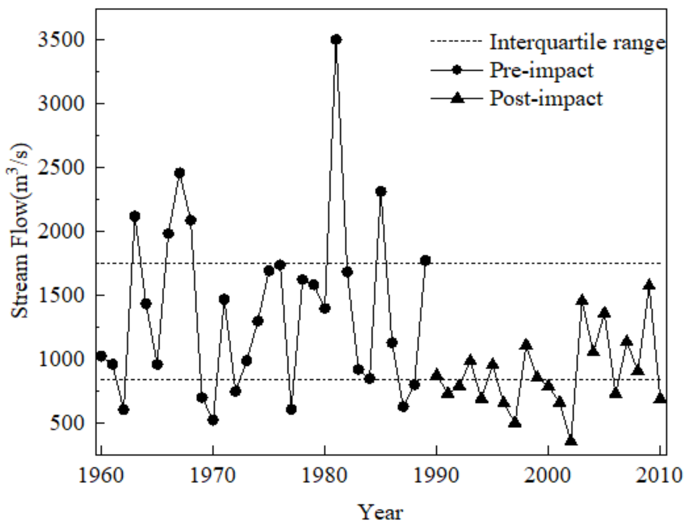


Figure 1. Natural streamflow of September

The above-mentioned methods partly improved the assessment mainly by considering the multiple statistical characteristics of flow series rather than only the frequency of IHAs within a single range. Nevertheless, a time series is a sequence taken at successive equally spaced points in time in which order does matter. It has not only statistical characteristics but also morphological characteristics which depict the shape of the time series' graph (how the time series changes with time). Unlike the "morphology of river" which is the shape of the waterbody, the "morphology of time series" depicts how the time series varies with the time [*Syed et al.,* 2008; *Sung et al.,* 2009]. In the field of hydrology, flow data and IHAs all belong to time series which have morphological characteristics. Thus in this work, we only focus on the "morphology of hydrological time series" and the alteration of morphological characteristics of IHAs is a reflection of flow regime changes in terms of the process of river flow [*Araújo et al.,* 2006, 2010]. Take indices in the fourth group of IHAs (Table 1) as an example, the high and low pulses

*accepted version: https://doi.org/10.1007/s00477-020-01926-6*

count the frequency of the extreme-flow events within a year. The frequency of extreme flows varies from year to year and their impacts on ecosystems are also different. This kind of fluctuation has strong impacts on the river ecosystem as it may change river morphology and affect aquatic productivity [*Bunn et al.*, 2002; *Woodward et al.*, 2016]. Previous studies indicated the fact that high-flow events will lead to erosions and increase difficulties for the inhabitation of aquatic creatures due to its high water speed [*Bednarek et al.*, 2001, *Trinci et al.*, 2017]. On the contrary, low-flow events lead to an increase of sediment and algae in river [*Oliver et al.*, 2014; *Mendoza-Lera et al.*, 2016]. The fluctuation in the frequency of extreme-flow events from one year to the next also matters as continuous years with numerous extreme-flow events have different impacts on river compared with intermittent ones [*Kozlowski et al.*, 2002; *Costigan et al.*, 2017]. While the sequence, which indicates a morphological characteristic of the flow regimes, cannot be represented in IHA index nor the RVA method. Therefore, there is a need to consider the morphological characteristics of each IHA for a comprehensive assessment of hydrological alteration, which has rarely been studied before.

This study aims to: 1) propose a revised RVA that can reflect the morphological characteristics of IHAs. 2) apply the traditional and revised RVAs to assess the hydrological alteration of the upper Yellow River; 3) compare the results of the traditional and revised RVAs for verifying the advantage of the new method.

## 2 Methodology

The revised RVA contains 5 steps:1) calculate the indicators of hydrological alteration 2) calculate the frequency alteration of IHAs; 3) assess the morphological alteration of the IHAs between the pre-impact and post-impact periods; 4) estimate an overall hydrological alteration by

*accepted version: https://doi.org/10.1007/s00477-020-01926-6*

combining the frequency and morphological alterations; and 5) identify the degree of the alteration in hydrological regime. The details of each step are presented as follows.

## 2.1 Calculation of the indicators of hydrological alteration

The IHAs are first introduced by *Richter et al.* [1996] and can be categorized into five groups. The first group measures the flow magnitude using the monthly average flow for each month (Table 1). The second group measures the extreme status with the flow minimums and maximums from moving averages for the specific length (e.g., 1-, 3-, 7-, 30-, and 90-day) across each year. The base flow index is calculated as the ratio of 7-day minimum to annual average flow. The parameters in the third group record the timing (Julian date) of extreme flow (1-day minimums and maximums). High and low pulses in the fourth group are defined as the occurrence and lasting time of days of an event when daily streamflow is larger than the 75th percentile discharge (high pulse) or less than the 25th percentile discharge (low pulse) within a year. The number of the high pulses (Yellow zones) is 3 in an example discharge series in Figure 2, while the number of the low pulses (Blue zones) is 1. The mean duration of high (or low) pulses the average of the lasting days of those high (or low) pulse events. The rise and fall rates in the fifth group, measuring as the rate of changes in two consecutive days, are computed for each day within each year. As shown in Figure 3, the consecutive “rising” days are defined as a “rising period”. The number of reversals counts all the points that a “rising” or “falling” period shifts to another one. And in Figure 3, the number of reversals is 2.

*accepted version: https://doi.org/10.1007/s00477-020-01926-6*

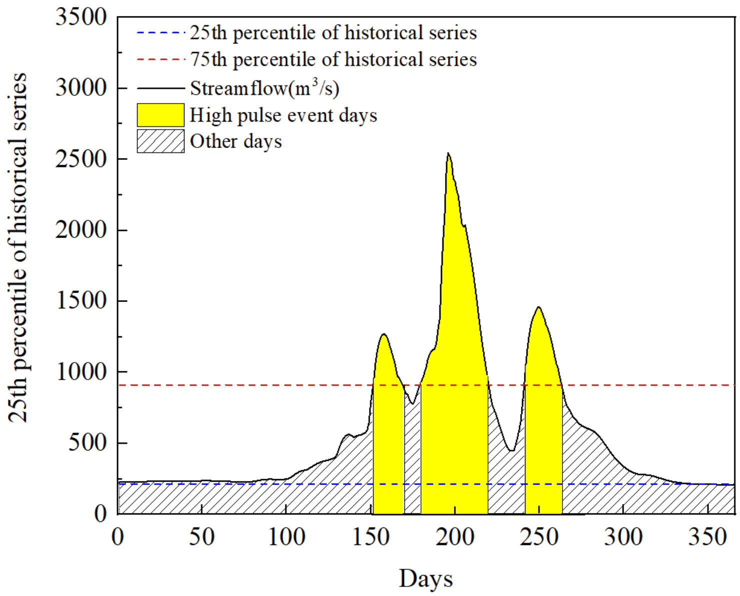


Figure 2. The definition for High pulse events. This figure is an example for one year. High pulses (yellow parts) are identified as those periods during which streamflow rise above the 75th percentile of the period.

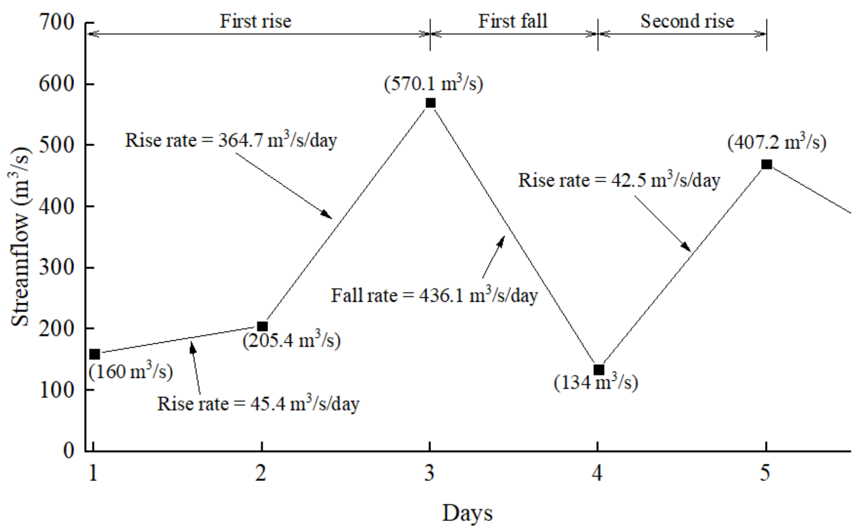


Figure 3. The definition for the 5th group IHAs. The rise (fall) rite is the mean rite of positive (negative) changes from one day to the next. The consecutive “rising (falling)” days is defined as “rising (falling) period”. The number of reversals counts all the points that a “rising” or “falling” period change to another one.

## 2.2 Assessment of frequency alteration of IHA time series

For all IHAs, the degree of frequency alteration $F_i$ ($i = 1,2,3,\cdots,32$) assessed by traditional RVA [*Richter et al.*, 1997] is expressed as:

$$F_i = \left|\frac{N_{oi} - N_{ei}}{N_{ei}}\right| \quad (1)$$

where $N_{oi}$ is the count of years when the $i^{th}$ IHA falling into RVA range in the post-impact period; while $N_{ei}$ is the expected number of years of the $i^{th}$ IHA falling into RVA range in the post-impact period. $N_{ei}$ is calculated by the number of values in RVA boundaries during pre-impact period multiplied by the ratio of post-impact years to pre-impact years.

### 2.3 Assessment of morphological alteration of IHA time series

There are many methods for calculating the diversity of two time series [*Milbourn et al.*, 1999; *Champely et al.*, 2002; *Pavan et al.*, 2004; *Ding et al.*, 2008; *Engen et al.*, 2011]. To our knowledge, a time series and its fluctuation process can be uniquely determined when the ordering position and magnitude of each element in the time series are given [*Lacasa et al.*, 2015]. Thus, to get the morphological alteration of the time series, it is essential to choose a method that can consider the ordering relationships and magnitude differences of all the elements. Previous studies proved this view of point by combining the measure of similarity of ordering relationships and magnitude differences for hydrograph and got better results [*Wendi et al.*, 2019]. *Todeschini et at.* [2016] proposed a diversity measure approach by comparing the multi-properties of sequence elements. This method has so far been widely applied for data comparisons that require the consideration of ordering relationships, such as the comparison between different DNAs.

There are two steps to obtain the morphological alteration of IHA: (1) define the Hasse matrices of IHA and (2) calculate the Hasse distance of Hasse matrices.

*Define Hasse matrix.* Suppose that $Q$ ($\boldsymbol{q}_1$, $\boldsymbol{q}_2$, …, $\boldsymbol{q}_n$) is a sequence of $n$ elements, and each element is a vector of $m$ variables (properties). Two elements $\boldsymbol{q}_i$ and $\boldsymbol{q}_j$ in $Q$ are comparable if there is $\boldsymbol{q}_i(k)>\boldsymbol{q}_j(k)$ or $\boldsymbol{q}_i(k)<\boldsymbol{q}_j(k)$ for all $m$ variables ($i$, $j$=1, 2, ..., $n$; $k$=1, 2, ..., $m$). When

$\boldsymbol{q}_i(k) > \boldsymbol{q}_j(k)$ for all $m$ variables, there is $\boldsymbol{q}_i > \boldsymbol{q}_j$. When $\boldsymbol{q}_i(k) < \boldsymbol{q}_j(k)$ for all variables, there is $\boldsymbol{q}_i < \boldsymbol{q}_j$. The mathematical way is expressed as:

$$\boldsymbol{q}_i > \boldsymbol{q}_j \Leftrightarrow \boldsymbol{q}_i(k) > \boldsymbol{q}_j(k) \quad \forall k \in [1, m] \tag{2}$$

The Hasse matrix ($H$) of a sequence $Q$ is defined by comparing each two elements:

$$H_{ij} = \begin{cases} +1 & \text{if } \boldsymbol{q}_i(k) > \boldsymbol{q}_j(k) \quad \forall\, k \in [1, m] \\ -1 & \text{if } \boldsymbol{q}_i(k) < \boldsymbol{q}_j(k) \quad \forall\, k \in [1, m] \\ 0 & \text{otherwise} \end{cases} \tag{3}$$

The original Hasse matrix is an $n \times n$ antisymmetric matrix consisting only of 0 and $\pm 1$. More information can be reflected by adding any property of the elements to the main diagonal of Hasse matrix. The Hasse matrix that compares multiple properties is like a fingerprint of the sequence.

In our work, the ordering positions ($k$=1) and magnitudes ($k$=2) of the elements are chosen as two variables ($m$=2) of the IHA to quantify the morphological characteristics. Sequence $Q(\boldsymbol{q}_1, \boldsymbol{q}_2, \ldots, \boldsymbol{q}_n)$ represents the selected IHA, $n$ stands for the number of the years chosen for comparison. For selected IHA, $\boldsymbol{q}_i(1)$ and $\boldsymbol{q}_i(2)$ means the ordering variable and magnitude variable in $i$th year. Considering that the ecosystem has a certain carrying capacity, the IHAs data was not used to determine the Hasse matrix directly but instead converted to three degrees. A hydrological time series is divided into three ranges by its RVA boundaries during the pre-impact period. Values in the range under the lower boundary is defined as low values, within the RVA boundaries as middle values and high values above the higher boundary [*Yang et al.,* 2010]. The elements in the time series falling into the low, middle and high value ranges are converted to 1, 2, and 3, respectively. Taking the data in Table 2 as an example. The RVA boundaries are 125.5 $m^3/s$ and 194.5 $m^3/s$ at the 25th and 75th percentiles of pre-impact January flow (165, 115, 194, 196, 129, 191; units: $m^3/s$). Hence, the pre-impact flow can be converted to

accepted version: https://doi.org/10.1007/s00477-020-01926-6

(2, 1, 2, 3, 2, 2). The post-impact flow (253, 126, 144, 172, 163, 128; units: $m^3/s$) can be converted to (3, 2, 2, 2, 2, 2) according to the defined boundaries. The ordering variable derives from the index of the time series. The lengths of pre- and post-impact periods are both 6, so both of their ordering sequences are (1, 2, 3, 4, 5, 6) (see the first column in Table 2). In this example, for the post-impact period, the converted magnitude variable ($\boldsymbol{q}_1(2)$) is 3 when the ordering variable ($\boldsymbol{q}_1(1)$) is 1, while the converted magnitude variable ($\boldsymbol{q}_2(2)$) is 2 when the ordering variable ($\boldsymbol{q}_2(1)$) is 2. By applying equation 3, $H_{12}$ and $H_{21}$ of the post-impact period are both 0. The Hasse matrices of the pre-impact and post-impact January flow obtained by comparing the ordering and magnitude variables are given in Figure 4. The magnitudes of IHAs are represented by $H_{ii} = \frac{p_i}{p_{max}}$ where $p_i$ is the $i^{th}$ converted IHA value and $p_{max}$ is the maximum of all converted IHAs, which substitutes the diagonal elements of Hasse Matrix.

Table 2. Ordering and magnitude variables of January flow

| Ordering variable | Magnitude variable | | | |
|---|---|---|---|---|
| | Row value ($m^3/s$) | | Converted value | |
| ID | Pre-impact | Post-impact | Pre-impact | Post-impact |
| 1 | 165 | 253 | 2 | 3 |
| 2 | 115 | 126 | 1 | 2 |
| 3 | 194 | 144 | 2 | 2 |
| 4 | 196 | 172 | 3 | 2 |
| 5 | 129 | 163 | 2 | 2 |
| 6 | 191 | 128 | 2 | 2 |

*accepted version: https://doi.org/10.1007/s00477-020-01926-6*

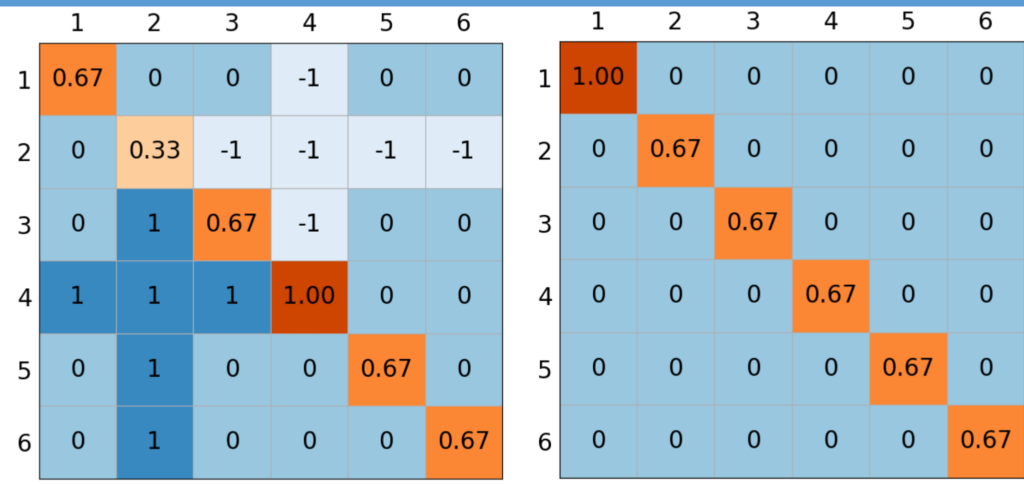


(a) Pre-impact January Flow (b) Post-impact January Flow

Figure 4. Hasse Matrices of pre- and post-impact January flow

*Compute Hasse distance.* Given a $n \times n$ pre-impact matrix $H^{pre}$ and a $n \times n$ post-impact matrix $H^{post}$, the Hasse distance of the two matrices $D_H(pre,post)$ is defined by:

$$D_H(pre, post) = (1-w) \cdot D_O(pre, post) + w \cdot D_D(pre, post) \tag{4}$$

where,

$$D_D(pre, post) = \frac{\sum_{i=0}^{n} \left| H_{ii}^{pre} - H_{ii}^{post} \right|}{n} \tag{5}$$

$$D_O(pre, post) = \frac{\sum_{i=1}^{n-1} \sum_{j=i+1}^{n} \left| H_{ij}^{pre} - H_{ij}^{post} \right|}{n \cdot (n-1)/2} \tag{6}$$

where $D_D$ is the distance due to the diagonal elements of the two matrices, while $D_O$ is the distance due to the off-diagonal elements. The summations of diagonal elements and off-diagonal elements cannot be greater than $n$ and $n \cdot (n-1)/2$, respectively. The resulting $D_D$ and $D_O$ fall into the range from 0 to 1. $w$ has a range of [0,1] and is a weighting parameter determined by the importance of ordering relationships and magnitude differences. Therefore, the range of the

accepted version: https://doi.org/10.1007/s00477-020-01926-6

Hasse distance is between 0 and 1. A decrease in Hasse distance implies a higher similarity between two time series.

*Hasse distance between matrices of different sizes.* The above method is only applicable to the matrices of the same size. An adaptive process is needed when the lengths of two datasets are different.

Suppose that the numbers of pre-impact and post-impact years are $n_1$ and $n_2$ ($n_1 > n_2$), and associated Hasse matrices are denoted as $H_1$ and $H_2$. The sizes of $H_1$ and $H_2$ are $n_1 \times n_1$ and $n_2 \times n_2$, respectively. The Hasse distance between $H_1$ and $H_2$ can be calculated by comparing $n_1 - n_2 + 1$ times the overlapping part of these two matrices, moving the smaller matrix diagonally from the top-left corner to the bottom-right corner of the bigger one. The smallest distance among the $n_1 - n_2 + 1$ distances is the Hasse distance between $H_1$ and $H_2$. In this way, the most similar part between pre-impact and post-impact datasets can be found.

## 2.4 Assessment of Overall Alteration

The overall alteration of *ith* IHA ($OA_i$) is a combination of the frequency alteration $F_i$ and the morphological alteration $D_{Hi}$. The $OA_i$ should be no less than $F_i$ or $D_{Hi}$, and the frequency and morphological alterations should contribute evenly to the overall alteration [*Yang et al.* 2014]. The integration of $F_i$ and $D_{Hi}$ into $OA_i$ is:

$$OA_i = 1 - (1 - F_i)(1 - D_{Hi}) \quad (7)$$

The overall alteration has the following five properties: (1) ranges from 0 and 1; (2) increases with the increase of $F_i$ or $D_{Hi}$; (3) equals to 1 if $F_i$ or $D_{Hi}$ is 1; (4) not equals to 0 if either $F_i$ or $D_{Hi}$ is not 1, (5) the frequency and morphological alterations are of equal importance.

The total overall alteration can be calculated by [*Richter et al.* 1998]:

*accepted version: https://doi.org/10.1007/s00477-020-01926-6*

$$OA = \frac{1}{32}\sum_{i=1}^{32} OA_i \quad (8)$$

### 2.5 Degree of the Hydrological Alteration

In this work, the alteration of IHAs changed by 0%, 0%-33%, 33%-67%, and above 67% are defined as no, low, medium, and high alteration, respectively (e.g. *Xue et al.*, 2017).

## 3 Study Area

The Yellow River is one of the longest rivers in the world and supplies more than 100 million people. Located in the upper part of the Yellow River, the catchment controlled by Lanzhou station is the main water source of the Yellow River (Figure 5). The local ecosystem is very fragile due to the special location [*Feng et al.,* 2006; *Wang et al.,* 2017, 2018]. In recent years, the hydrological regime of the upper Yellow River has been changed a lot. It is reported that the sand content of the Yellow River is decreasing [*Wu et al.,* 2015; *Yao et al.,* 2016]. The inhabitants in Lanzhou also said that the river was not as fierce as before. All these phenomena show an obvious change in the flow regime of the river.

*accepted version: https://doi.org/10.1007/s00477-020-01926-6*

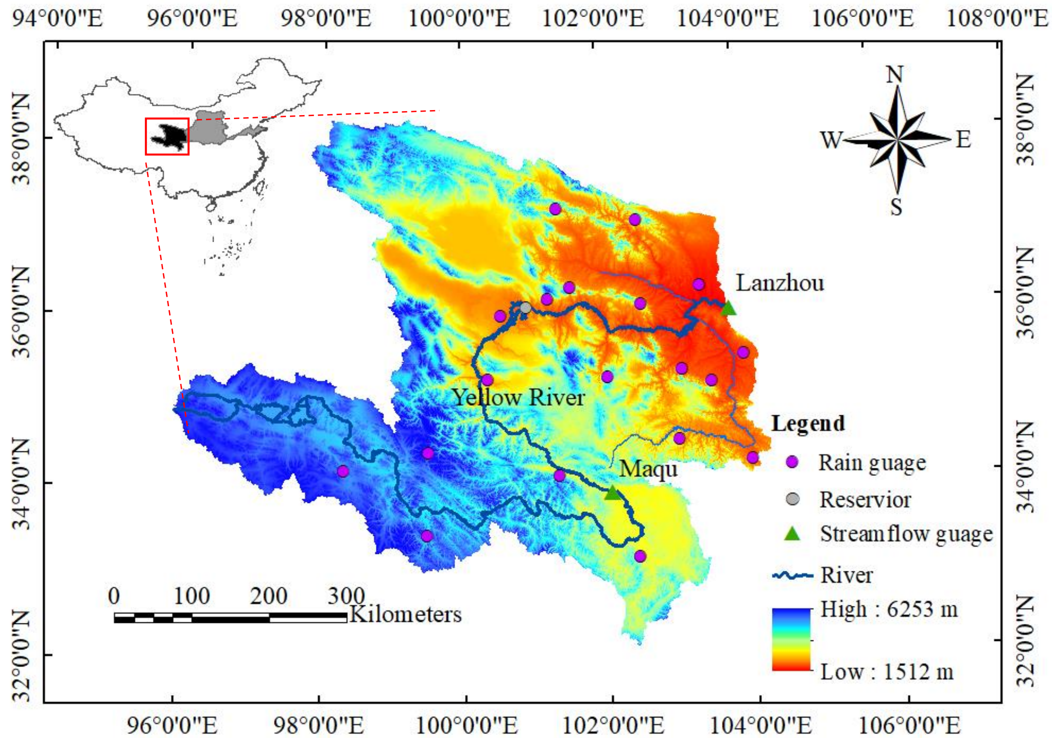


Figure 5. Location map of study area on the upper Yellow River

It's known that human activities, especially dam construction and operation, will change the fluctuation of river discharge compared with the pre-impact period [*Yang et al.,* 2008]. The impact on river flow can be more significant than the influence derived from climate change. Thus, the flow data of Lanzhou station which is located downstream of Longyangxia dam is chosen to investigate the morphological alterations. Longyangxia reservoir, the first large reservoir on the Yellow River in location, is located at 154 km upstream from Lanzhou station. Its storage capacity and dam height are $247\times10^8$ $m^3$ and 178 m, respectively. *Yu et al.* [2010] found that the construction and operation of Longyangxia Dam have a significant influence on the river eco-environment. The hydrological alteration of Lanzhou station is influenced by both climate change and human activities. To test the robustness of the new method and analysis the difference in morphological alteration caused only by climate change, another station named Maqu which is located upstream of the dam.

Daily streamflow data from 1967 to 2005 of Lanzhou and Maqu stations were collected to compare the difference in the morphological alterations with and without human activities. The whole period was divided into pre-, under-, and post-construction periods (1967-1977, 1978-1989, 1990-2005, respectively) based on the progress of the dam construction.

## 4 Results and Discussions

Considering the local ecosystem of upper Yellow river is very fragile, we set the RVA boundaries as the median plus or minus 17 percent [*Yang et al.* 2017]. This means only the IHA values falling in the range of the 34th to 67th percentiles will be counted in traditional RVA method.

### 4.1 Flow regime at two gauges

The flow data at Maqu and Lanzhou were plotted and compared (Figure 6). The maximum and minimum daily flow of the post-construction period are chosen as the thresholds to determine if the flow was significantly changed after the dam construction. In Figure 6, the number of the peaks above the maximum daily flow threshold (peaks in red rectangles) is greater than that of Maqu Station. Moreover, the magnitudes of flow peaks in 1990−2005 of Lanzhou station are much lower than that in the period from 1967 to 1989. This reveals the fact that the dam will reduce the peak flow of floods to prevent flood disasters. Thus, there do have morphological alterations in the flow regime of these two gauges after the dam construction and the alterations apparently differ.

accepted version: https://doi.org/10.1007/s00477-020-01926-6

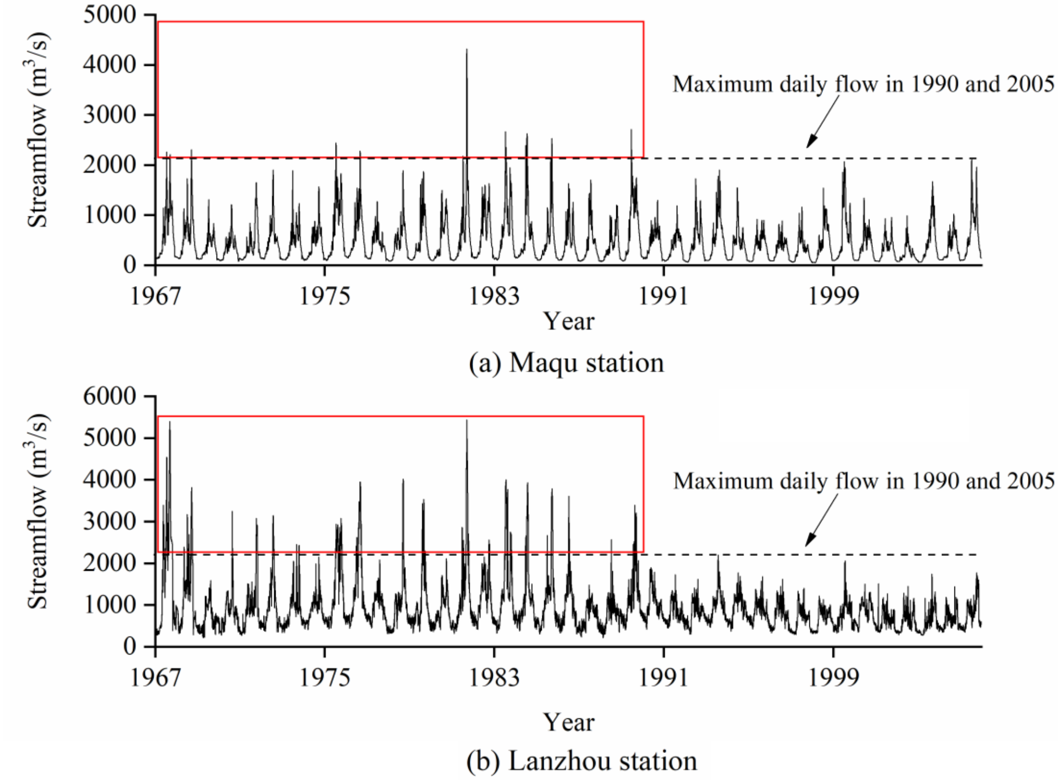


Figure 6. Hydrological process of Maqu (a) and Lanzhou (b). The maximum daily flow in 1990 and 2005 is chosen as the threshold of extreme flow events.

## 4.2 Calculation of RVA and the new revised method

To test the performance of the new method, the hydrological alteration of the upper Yellow river was calculated by traditional RVA and the one established in this study. The frequency alteration, morphological alteration, and overall alteration of Maqu and Lanzhou stations for all 32 IHAs are listed in Tables 3 for Maqu station and 4 for Lanzhou station.

*accepted version: https://doi.org/10.1007/s00477-020-01926-6*

Table 3. Hydrological alteration of the Maqu station

| IHAs | Pre-impact | Post-impact | | | | RVA boundaries | | Hydrological alteration | | | | | |
|---|---|---|---|---|---|---|---|---|---|---|---|---|---|
| | | Under-construction | | Post-construction | | | | Under-construction | | | Post-construction | | |
| | Median | Median | RD (%) | Median | RD (%) | Low | High | *F* | $D_H$ | *OA* | *F* | $D_H$ | *OA* |
| Group 1 (m$^3$/s) | | | | | | | | | | | | | |
| January | 123.00 | 101.00 | -17.89 | 87.00 | -29.27 | 117.80 | 136.50 | 0.82 | 0.40 | 0.89 | 1.00 | 0.27 | 1.00 |
| February | 129.50 | 102.30 | -21.00 | 89.38 | -30.98 | 112.50 | 132.80 | 0.82 | 0.42 | 0.89 | 1.00 | 0.27 | 1.00 |
| March | 174.00 | 146.50 | -15.80 | 109.50 | -37.07 | 148.60 | 185.40 | 0.08 | 0.27 | 0.33 | 0.86 | 0.39 | 0.92 |
| April | 234.50 | 243.30 | 3.75 | 220.80 | -5.84 | 212.80 | 323.10 | 0.47 | 0.30 | 0.63 | 0.04 | 0.20 | 0.23 |
| May | 418.00 | 331.00 | -20.81 | 373.50 | -10.65 | 371.50 | 484.10 | 0.63 | 0.40 | 0.78 | 0.59 | 0.25 | 0.69 |
| June | 625.00 | 545.80 | -12.67 | 511.50 | -18.16 | 582.10 | 715.60 | 1.00 | 0.40 | 1.00 | 0.73 | 0.30 | 0.81 |
| July | 749.00 | 1071.00 | 42.99 | 622.50 | -16.89 | 554.20 | 1109.00 | 0.08 | 0.35 | 0.40 | 0.04 | 0.17 | 0.20 |
| August | 558.00 | 694.50 | 24.46 | 622.50 | 11.56 | 511.10 | 754.40 | 0.10 | 0.36 | 0.43 | 0.18 | 0.17 | 0.32 |
| September | 842.00 | 1120.00 | 33.02 | 605.80 | -28.05 | 509.80 | 1155.00 | 0.28 | 0.31 | 0.51 | 0.38 | 0.13 | 0.46 |
| October | 782.00 | 806.00 | 3.07 | 557.00 | -28.77 | 555.10 | 847.80 | 0.08 | 0.40 | 0.45 | 0.18 | 0.22 | 0.36 |
| November | 361.00 | 342.30 | -5.18 | 291.50 | -19.25 | 276.20 | 395.80 | 0.08 | 0.40 | 0.45 | 0.24 | 0.24 | 0.42 |
| December | 144.00 | 145.00 | 0.69 | 102.40 | -28.89 | 126.80 | 171.10 | 0.10 | 0.36 | 0.42 | 0.31 | 0.20 | 0.45 |
| Group 2 (m$^3$/s) | | | | | | | | | | | | | |
| 1-day min. | 100.00 | 93.40 | -6.60 | 80.30 | -19.70 | 97.40 | 115.20 | 0.45 | 0.29 | 0.61 | 1.00 | 0.27 | 1.00 |
| 3-day min. | 105.00 | 93.40 | -11.05 | 82.28 | -21.64 | 98.91 | 115.90 | 0.45 | 0.36 | 0.65 | 1.00 | 0.28 | 1.00 |
| 7-day min. | 106.70 | 93.59 | -12.29 | 83.51 | -21.73 | 106.30 | 119.00 | 1.00 | 0.33 | 1.00 | 1.00 | 0.28 | 1.00 |
| 30-day min. | 114.40 | 98.49 | -13.91 | 86.38 | -24.49 | 110.60 | 127.80 | 0.82 | 0.38 | 0.89 | 0.86 | 0.24 | 0.90 |
| 90-day min. | 141.30 | 116.70 | -17.41 | 101.60 | -28.10 | 127.30 | 163.10 | 0.63 | 0.45 | 0.80 | 0.86 | 0.34 | 0.91 |
| 1-day max. | 1890.00 | 1880.00 | -0.53 | 1320.00 | -30.16 | 1560.00 | 2261.00 | 0.08 | 0.38 | 0.44 | 0.31 | 0.26 | 0.49 |
| 3-day max. | 1793.00 | 1832.00 | 2.18 | 1262.00 | -29.62 | 1529.00 | 2199.00 | 0.08 | 0.38 | 0.44 | 0.31 | 0.26 | 0.49 |
| 7-day max. | 1593.00 | 1705.00 | 7.03 | 1145.00 | -28.12 | 1506.00 | 2083.00 | 0.27 | 0.42 | 0.57 | 0.31 | 0.26 | 0.49 |
| 30-day max. | 1330.00 | 1285.00 | -3.38 | 829.50 | -37.63 | 926.80 | 1512.00 | 0.28 | 0.44 | 0.60 | 0.18 | 0.31 | 0.43 |

*accepted version: https://doi.org/10.1007/s00477-020-01926-6*

| | | | | | | | | | | | | | |
|---|---|---|---|---|---|---|---|---|---|---|---|---|---|
| 90-day max. | 870.50 | 1076.00 | 23.61 | 684.60 | -21.36 | 723.40 | 988.10 | 0.27 | 0.39 | 0.56 | 0.73 | 0.29 | 0.81 |
| Baseflow index | 0.25 | 0.21 | -16.00 | 0.22 | -12.00 | 0.24 | 0.27 | 0.82 | 0.35 | 0.88 | 0.59 | 0.26 | 0.69 |
| Group 3 (Julian date) | | | | | | | | | | | | | |
| Date of min. | 16.00 | 17.00 | 6.25 | 7.50 | -53.13 | 39.52 | 335.00 | 0.63 | 0.34 | 0.76 | 0.59 | 0.27 | 0.70 |
| Date of max. | 207.00 | 225.00 | 8.70 | 197.00 | -4.83 | 195.80 | 245.60 | 0.08 | 0.30 | 0.36 | 0.31 | 0.31 | 0.52 |
| Group 4 | | | | | | | | | | | | | |
| Low pulse count | 2.00 | 2.00 | 0.00 | 2.00 | 0.00 | 1.00 | 3.00 | 0.29 | 0.28 | 0.49 | 0.07 | 0.15 | 0.21 |
| Low pulse duration (day) | 63.75 | 10.50 | -83.53 | 60.25 | -5.49 | 39.29 | 89.99 | 0.54 | 0.42 | 0.74 | 0.20 | 0.29 | 0.43 |
| High pulse count | 3.00 | 3.50 | 16.67 | 3.00 | 0.00 | 3.00 | 5.04 | 0.22 | 0.35 | 0.50 | 0.20 | 0.10 | 0.28 |
| High pulse duration (day) | 12.00 | 30.75 | 156.25 | 10.50 | -12.50 | 8.92 | 16.08 | 0.82 | 0.42 | 0.89 | 0.59 | 0.21 | 0.67 |
| Group 5 | | | | | | | | | | | | | |
| Rise rate ($m^3/s$) | 13.50 | 12.75 | -5.56 | 10.75 | -20.37 | 11.96 | 14.24 | 0.45 | 0.44 | 0.69 | 0.31 | 0.26 | 0.49 |
| Fall rate ($m^3/s$) | -11.50 | -13.50 | 17.39 | -10.50 | -8.70 | -15.04 | -10.48 | 0.10 | 0.49 | 0.54 | 0.10 | 0.25 | 0.33 |
| Number of reversals | 85.00 | 86.50 | 1.76 | 80.00 | -5.88 | 77.84 | 87.28 | 0.45 | 0.40 | 0.67 | 0.45 | 0.38 | 0.66 |
| Total overall alteration | | | | | | | | 0.42 | 0.38 | 0.63 | 0.48 | 0.25 | 0.60 |

* RD, relative difference; *F*, frequency alteration; $D_H$, Hasse distance; *OA*, overall alteration.

*accepted version: https://doi.org/10.1007/s00477-020-01926-6*

Table 4. Hydrological alteration of Lanzhou station

| IHAs | Pre-impact | Post-impact | | | | RVA boundaries | | Hydrological alteration | | | | | |
|---|---|---|---|---|---|---|---|---|---|---|---|---|---|
| | | Under-construction | | Post-construction | | | | Under-construction | | | Post-construction | | |
| | Median | Median | RD (%) | Median | RD (%) | Low | High | *F* | $D_H$ | *OA* | *F* | $D_H$ | *OA* |
| Group 1 ($m^3/s$) | | | | | | | | | | | | | |
| January | 525.00 | 599.00 | 14.10 | 452.50 | -13.81 | 372.90 | 640.50 | 0.83 | 0.38 | 0.90 | 0.24 | **0.36** | 0.51 |
| February | 487.50 | 463.80 | -4.86 | 444.80 | -8.76 | 353.20 | 566.30 | 0.28 | 0.40 | 0.57 | 0.10 | **0.40** | 0.46 |
| March | 526.00 | 496.00 | -5.70 | 434.50 | -17.40 | 435.20 | 531.10 | 0.28 | **0.32** | 0.52 | 0.31 | 0.27 | 0.50 |
| April | 708.50 | 695.50 | -1.83 | 598.80 | -15.48 | 576.20 | 776.10 | 0.28 | 0.25 | 0.47 | 0.45 | **0.26** | 0.59 |
| May | 1190.00 | 1050.00 | -11.76 | 1110.00 | -6.72 | 1037.00 | 1221.00 | 0.10 | 0.29 | 0.36 | 0.24 | **0.24** | 0.42 |
| June | 1170.00 | 1045.00 | -10.68 | 912.50 | -22.01 | 1061.00 | 1377.00 | 0.45 | **0.41** | 0.67 | 0.86 | 0.36 | 0.91 |
| July | 1180.00 | 1485.00 | 25.85 | 909.50 | -22.92 | 1109.00 | 2026.00 | 0.08 | **0.46** | 0.50 | 0.31 | **0.29** | 0.51 |
| August | 1450.00 | 1355.00 | -6.55 | 891.00 | -38.55 | 1154.00 | 1522.00 | 0.27 | **0.45** | 0.60 | 0.73 | **0.28** | 0.80 |
| September | 1100.00 | 1278.00 | 16.18 | 813.30 | -26.06 | 1005.00 | 2107.00 | 0.10 | **0.35** | 0.42 | 0.59 | **0.27** | 0.70 |
| October | 976.00 | 1365.00 | 39.86 | 865.50 | -11.32 | 829.70 | 1291.00 | 0.63 | 0.39 | 0.78 | 0.10 | **0.27** | 0.34 |
| November | 741.50 | 835.80 | 12.72 | 802.00 | 8.16 | 676.90 | 856.10 | 0.08 | 0.34 | 0.40 | 0.24 | **0.29** | 0.46 |
| December | 578.00 | 612.00 | 5.88 | 552.50 | -4.41 | 492.70 | 636.20 | 0.27 | **0.48** | 0.62 | 0.18 | **0.33** | 0.45 |
| Group 2 ($m^3/s$) | | | | | | | | | | | | | |
| 1-day min. | 313.00 | 321.00 | 2.56 | 338.50 | 8.15 | 278.80 | 341.60 | 0.10 | **0.44** | 0.49 | 0.04 | **0.38** | 0.41 |
| 3-day min. | 356.70 | 330.70 | -7.29 | 349.70 | -1.96 | 281.60 | 385.90 | 0.10 | **0.50** | 0.55 | 0.38 | **0.41** | 0.63 |
| 7-day min. | 375.40 | 351.10 | -6.47 | 359.00 | -4.37 | 304.50 | 433.60 | 0.28 | **0.40** | 0.57 | 0.38 | **0.42** | 0.64 |
| 30-day min. | 426.40 | 441.50 | 3.54 | 396.30 | -7.06 | 354.90 | 466.90 | 0.10 | **0.45** | 0.50 | 0.04 | **0.36** | 0.38 |
| 90-day min. | 512.30 | 508.90 | -0.66 | 449.00 | -12.36 | 459.90 | 557.50 | 0.08 | 0.44 | 0.49 | 0.73 | **0.48** | 0.86 |
| 1-day max. | 3080.00 | 3570.00 | 15.91 | 1650.00 | -46.43 | 2438.00 | 3273.00 | 0.63 | 0.27 | 0.73 | 1.00 | **0.28** | 1.00 |
| 3-day max. | 2983.00 | 3485.00 | 16.83 | 1430.00 | -52.06 | 2371.00 | 3147.00 | 0.63 | 0.27 | 0.73 | 1.00 | **0.28** | 1.00 |
| 7-day max. | 2884.00 | 3284.00 | 13.87 | 1301.00 | -54.89 | 2140.00 | 3029.00 | 0.82 | 0.24 | 0.86 | 1.00 | **0.28** | 1.00 |
| 30-day max. | 2452.00 | 2857.00 | 16.52 | 1164.00 | -52.53 | 1438.00 | 2709.00 | 0.45 | 0.25 | 0.59 | 0.59 | 0.22 | 0.68 |

*accepted version: https://doi.org/10.1007/s00477-020-01926-6*

| | | | | | | | | | | | | | |
|---|---|---|---|---|---|---|---|---|---|---|---|---|---|
| 90-day max. | 1556.00 | 1904.00 | 22.37 | 1053.00 | -32.33 | 1250.00 | 2189.00 | 0.47 | **0.41** | 0.68 | 0.73 | **0.32** | 0.81 |
| Baseflow index | 0.35 | 0.36 | 2.86 | 0.49 | 40.00 | 0.34.00 | 0.42 | 0.10 | **0.44** | 0.49 | 1.00 | **0.47** | 1.00 |
| Group 3 (Julian date) | | | | | | | | | | | | | |
| Date of min. | 37.00 | 49.50 | 33.78 | 65.00 | 75.68 | 45.64 | 104.70 | 0.47 | 0.33 | 0.64 | 0.51 | 0.26 | 0.64 |
| Date of max. | 248.00 | 240.50 | -3.02 | 208.00 | -16.13 | 231.70 | 263.10 | 0.27 | 0.23 | 0.43 | 0.73 | 0.31 | 0.81 |
| Group 4 | | | | | | | | | | | | | |
| Low pulse count | 9.00 | 10.50 | 16.67 | 12.50 | 38.89 | 6.00 | 10.04 | 0.21 | 0.27 | 0.43 | 0.71 | **0.34** | 0.81 |
| Low pulse duration (day) | 2.50 | 2.50 | 0.00 | 2.00 | -20.00 | 2.00 | 3.12 | 0.08 | 0.40 | 0.45 | 0.54 | 0.20 | 0.63 |
| High pulse count | 5.00 | 8.50 | 70.00 | 6.50 | 30.00 | 4.00 | 10.04 | 0.38 | 0.20 | 0.50 | 0.26 | **0.31** | 0.49 |
| High pulse duration (day) | 5.50 | 2.75 | -50.00 | 1.25 | -77.27 | 2.48 | 21.88 | 0.10 | 0.21 | 0.29 | 0.59 | 0.21 | 0.67 |
| Group 5 | | | | | | | | | | | | | |
| Rise rate ($m^3/s$) | 43.00 | 53.25 | 23.84 | 48.50 | 12.79 | 39.96 | 47.56 | 1.00 | 0.35 | 1.00 | 0.45 | 0.23 | 0.58 |
| Fall rate ($m^3/s$) | -40.50 | -55.50 | 37.04 | -47.00 | 16.05 | -48.08 | -39.92 | 0.82 | 0.26 | 0.86 | 0.31 | 0.18 | 0.43 |
| Number of reversals | 167.00 | 191.00 | 14.37 | 214.00 | 28.14 | 159.70 | 177.20 | 0.82 | **0.44** | 0.90 | 1.00 | **0.46** | 1.00 |
| Total overall alteration | | | | | | | | 0.36 | 0.35 | 0.59 | 0.51 | 0.31 | 0.66 |

* RD, relative difference; *F*, frequency alteration; $D_H$, Hasse distance; *OA*, overall alteration. The bold numbers in Table 4 indicate the IHAs of Lanzhou that have large morphological alteration than Maqu.

accepted version: https://doi.org/10.1007/s00477-020-01926-6

*Analysis of the magnitude of monthly water conditions*

The frequency alterations of the average monthly flow at Maqu station in the first half-year before July are higher than that in the second half (see Table 3). And the most significant frequency alteration is 1.00 occurring in June over the under-construction period and in January and February during post-construction period. All the frequency alterations in the second half of the year are remaining low level except the one of September in post-construction period (0.38). For Lanzhou station, high values of frequency alteration of average monthly flow occur in summer (June and August) and winter (December to February) over the under-construction period (Figure 7). The most significant frequency alteration (0.63) occurs in January. As to the frequency alteration of the average monthly flow during the post-construction period, most high values are detected in summer and the highest value in June (0.86).

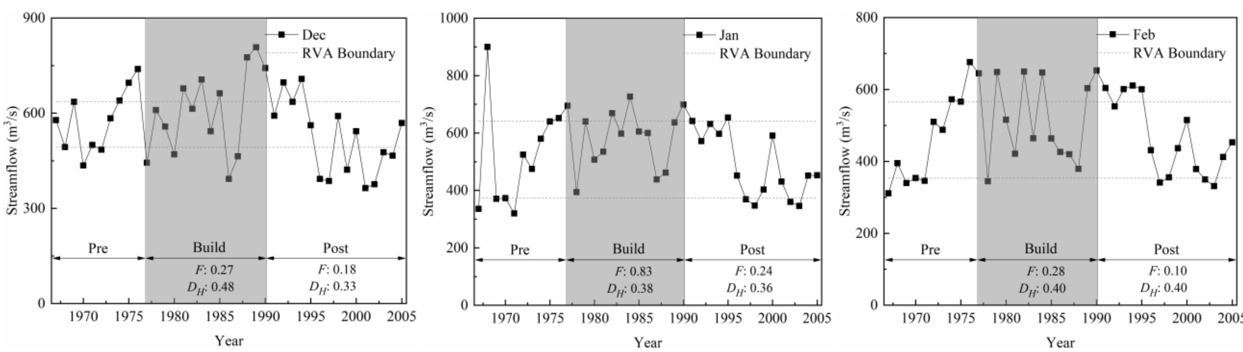


(a) December (b) January (c) February

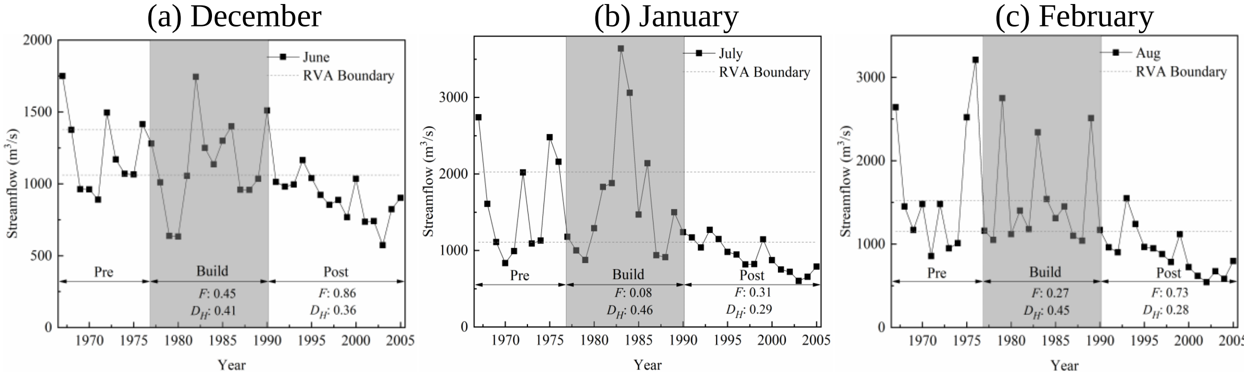


(d) June (e) July (f) August

Figure 7. Average monthly flow of winter (December (a), January (b), February (c)) and summer (June (d), July (e), August (f)) for Lanzhou station

*accepted version: https://doi.org/10.1007/s00477-020-01926-6*

For Maqu station, as to the under-construction period, the morphological alterations of average monthly flow are recognized as medium level for all months. Yet the post-construction period undergoes low morphological alterations of average monthly flow except in March that is defined as medium (0.39). The results of morphological alteration of Lanzhou station reveal that the dam shows the most considerable runoff regulation in summer and winter for both the under-construction and post-construction periods. Compared with the post-construction period, the dam has a lower impact on the magnitude of the average monthly flow from April to September, but a greater impact on the morphological characteristics of the average monthly flow is found all over the year (except April) during the under-construction period. It suggests that because the dam regulates river flow for electricity generation or irrigation, the flow regime has been changed a lot since the construction of the dam. The decrease in the monthly flow, especially during the summer, may lead to a degradation in aquatic habitats, a sharp increase in river water temperature and a significant reduction in dissolved oxygen. This accelerates the microbial decomposition of organic, reduces food supply to fish and invertebrates, and increases the mortality of fry [*Cui et al.,* 2018].

The highest and lowest overall alterations of Maqu occur in June (1.00) and March (0.33) during the under-construction period. In the post-construction period, the highest overall alteration occurs both in January (1.00) and February (1.00), while the lowest overall alteration happens in July (0.20). For Lanzhou station, the highest overall alterations of the under-construction period and post-construction period are found in January (0.90) and June (0.91), respectively. The lowest overall alterations of these two periods occur in May (0.36) and October (0.34), respectively.

*Analysis of the magnitude and duration of annual extreme water conditions*

For Maqu station, the frequency alterations of minimum flow are higher than the maximum flow for different durations. The frequency alterations of 7-day minimum flow in the under-

accepted version: https://doi.org/10.1007/s00477-020-01926-6

construction period and the 1-day, 3-day, 7-day minimum flows in the post-construction period reach 1.00 (see Figure 8 (a), (b), (c)). The 90-day minimum flow shows the most significant morphological alterations in both periods (see Figure 8 (d)). High or medium overall alterations are observed in both periods for all extreme discharge events.

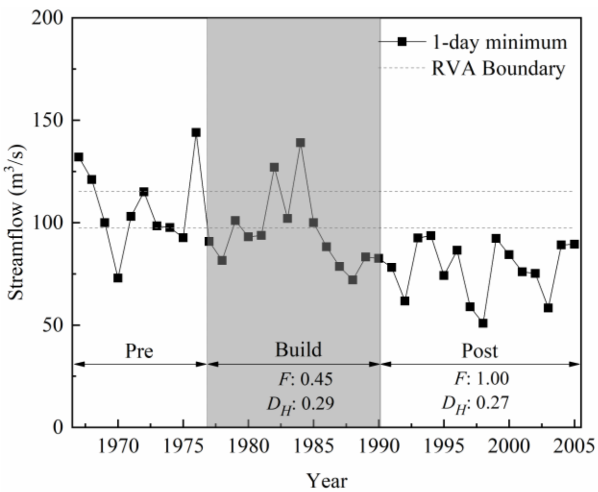


(a) 1-day minimum flow

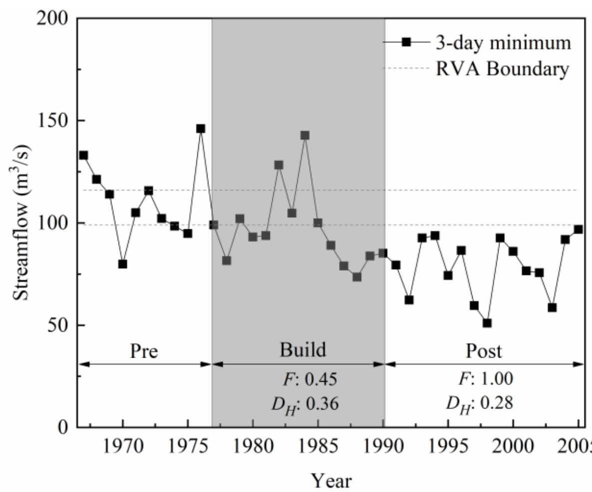


(b) 3-day minimum flow

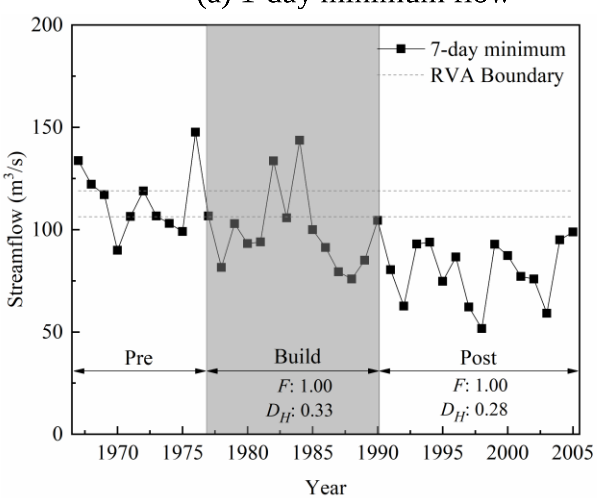


(c) 7-day minimum flow

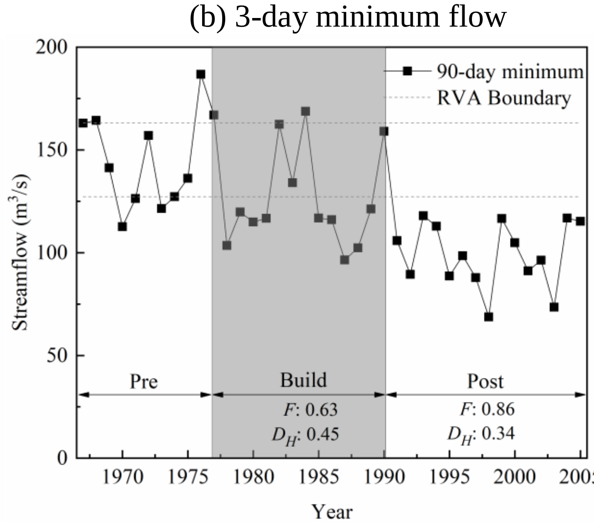


(d) 90-day minimum flow

Figure 8. Minimum flow of 1-day (a), 3-day (b), 7-day (c) and 90-day (d) for Maqu station

The frequency and morphological alterations show different patterns on the magnitude of extreme discharge events at Lanzhou station. The frequency alterations of minimum flow are relatively lower than that for the maximum flow for different durations. The 1-day minimum flow, 3-day minimum flow, 30-day minimum flow, and baseflow index show nearly no frequency alteration in the under-construction period (Figure 9). In contrast, the morphological alterations of

*accepted version: https://doi.org/10.1007/s00477-020-01926-6*

minimum flow are much higher than the maximum flow for different durations. Magnitudes for all morphological alterations of minimum flow are estimated as medium level, and all morphological alterations of maximum flow, except 90-day maximum which is defined as medium level in under-construction period, are defined as low change magnitude. High or medium overall alterations are observed in both periods for all extreme discharge events.

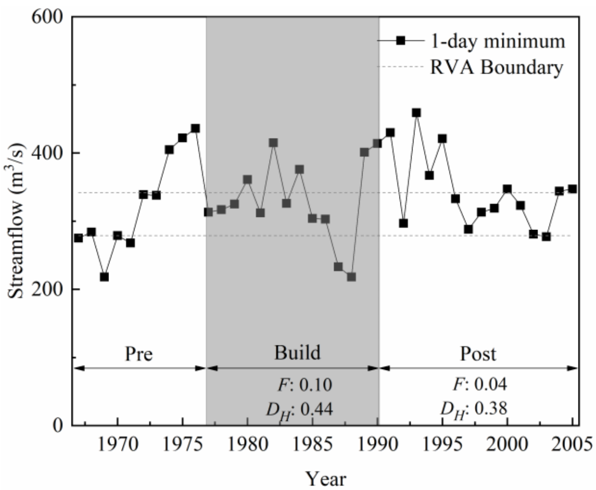


(a) 1-day minimum flow

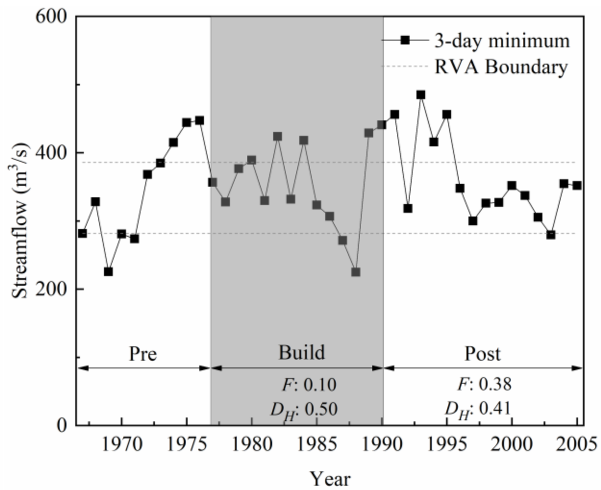


(b) 3-day minimum flow

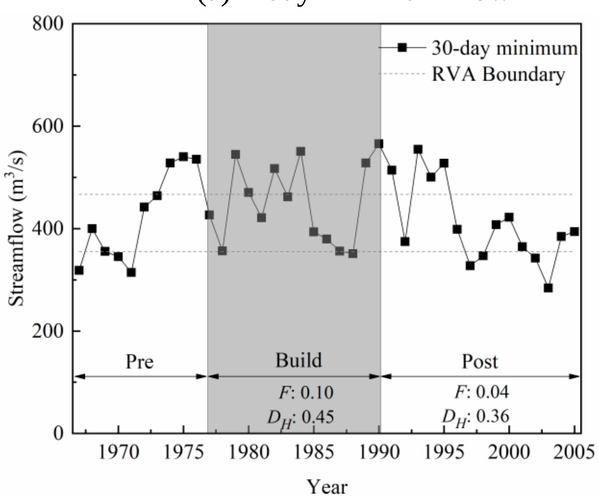


(c) 30-day minimum flow

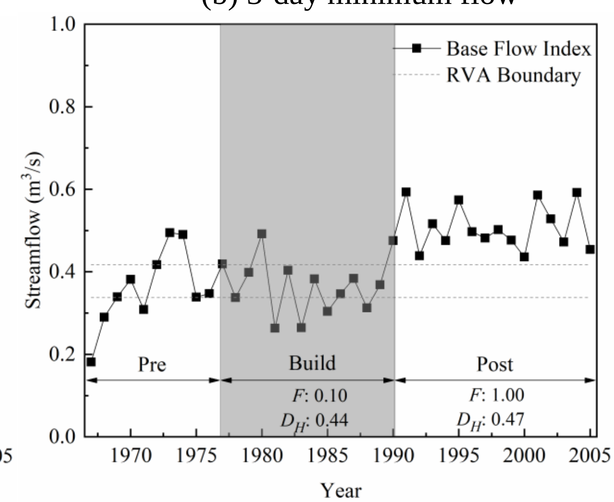


(d) Baseflow Index

Figure 9. Minimum flow of 1-day (a), 3-day (b), 30-day (c) and Baseflow Index (d) for Lanzou station

The above findings indicate the dam may reduce flood disasters and increase the volume of baseflow during its operation period. Moreover, the significant decline in extreme maximum flow will undermine the hydraulic connection between the river and floodplain, which reduces the nutrient and organic matter exchange between the river ecosystem and floodplain, resulting in insufficient nutrient supply for aquatic organisms.

*Analysis of the timing of annual extreme water conditions*

The median value of the Julian date of 1-day minimum flow at Maqu station delays 1 day in the under-construction period and advances 8.5 days in the post-construction period (Figure 10 (a)). Both the frequency and morphological alterations of this IHA in the under-construction period (0.63 and 0.34) are higher than those in the post-construction period (0.59 and 0.27). The median value of the Julian date of 1-day maximum flow at  Maqu station delays 18 days in the under-construction period and advances 10 days in the post-construction period (see Figure 11 (b)). The overall alteration of this IHA in the under- and post-construction periods are 0.36 and 0.52, respectively.

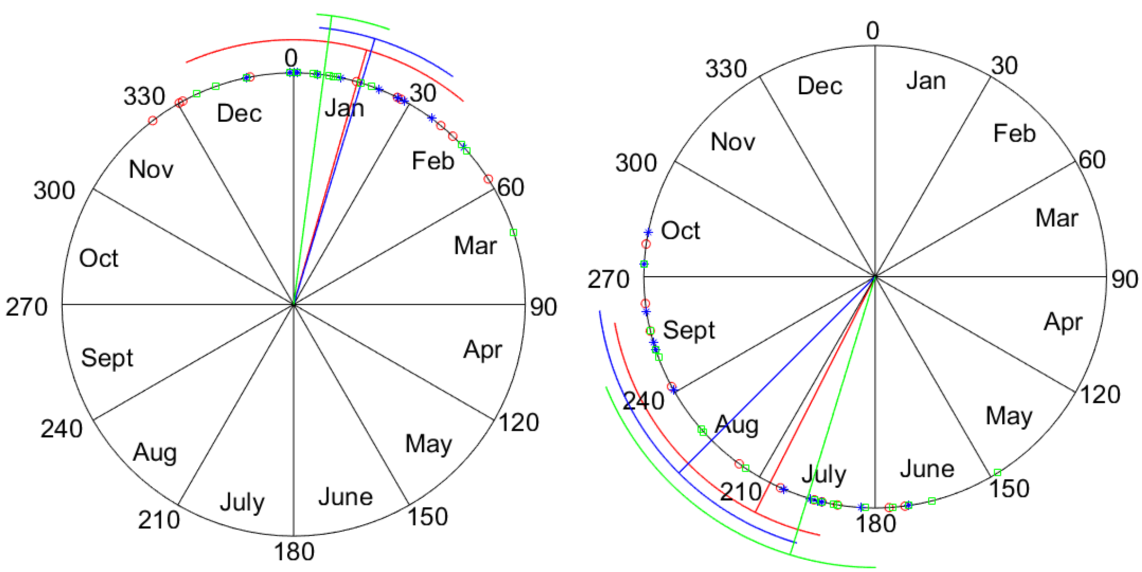


(a) Date of annual 1-day min. flow      (b) Date of annual 1-day max flow

Figure 10. Occurrence time of annual 1-day min. flow and 1-day max flow for Maqu station (Red, Blue, and Green: Pre-, Under- and Post construction period; Dots: occurrence time; Lines: median value; Curves: Interquartile range)

For Lanzhou station, the median value of the Julian date of 1-day minimum flow delays 12.5 days in the under-construction period and 28 days in the post-construction period (see Figure 11 (a)). Both periods present medium frequency alterations in this IHA. The frequency alteration in the under-construction period (0.47) is lower than that in the post-construction period (0.51). In contrast, the morphological alteration in the under-construction period (0.33) is higher than that in the post-construction period (0.26). The median value of the Julian date of 1-day maximum flow moves forward by 7.5 days in the under-construction period and 40 days in the post-construction period (see Figure 11 (b)). By considering the morphological alteration, the overall alteration is 0.43 (medium alteration) in the under-construction period and 0.81 (high alteration) in the post-construction period. The delays and advances of extremely high flow could affect the migration and reproduction of local fish, which may result in a reduction of the fish population.

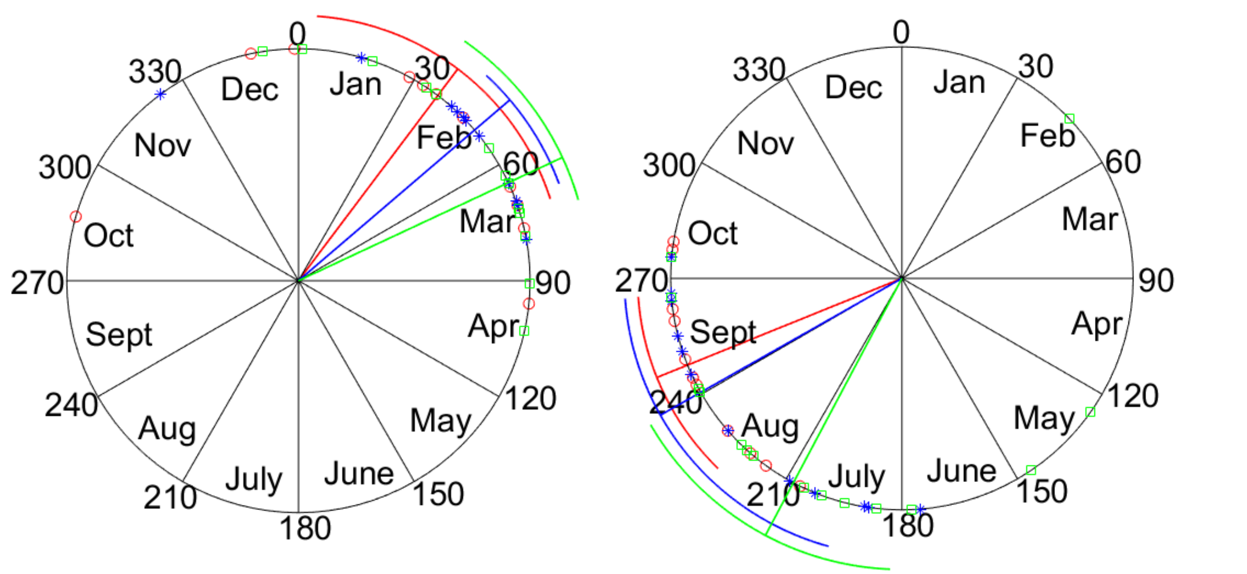


(a) Date of annual 1-day min. flow (b) Date of annual 1-day max flow

Figure 11. Occurrence time of annual 1-day min. flow and 1-day max flow for Lanzhou station (Red, Blue, and Green: Pre-, Under- and Post construction period; Dots: occurrence time; Lines: median value; Curves: Interquartile range)

*Analysis of the frequency and duration of high and low pulses*

The frequency and morphological alterations of the 4th group IHAs of Maqu station in the under-construction period are relatively higher than those in the post-construction period. High pulse duration shows the strongest frequency alterations both in under- and post-construction

accepted version: https://doi.org/10.1007/s00477-020-01926-6

periods (0.82 and 0.59, respectively). Low pulse duration shows the strongest morphological frequency alterations in both periods (0.42 and 0.29, respectively). High pulse duration shows the highest overall alterations in both periods (0.89 and 0.67).

For Lanzhou station, low pulse count and high pulse duration show nearly no frequency alterations (0.08 and 0.10) during the under-construction period. Low pulse count inversely presents high level frequency alterations during the post-construction period (0.71). Although the duration of low flow decreases after dam construction, the frequency of low flow shows an increase since the under-construction period (see Figure 12 (a)). Meanwhile, the frequency of high flow shows a significant increase and the duration of high flow shows a significant decrease (see Figure 12 (b) and median in Table 4). This implies that the construction of the dam breaks the continuity of flow events. The high flow process can effectively reduce the negative effects of low flow and provide nutrients to aquatic organisms. However, the decrease of high flow duration means that the high flow is not as effective in reducing the negative effect of low flow as before, which weakens the support of nutrients for aquatic life.

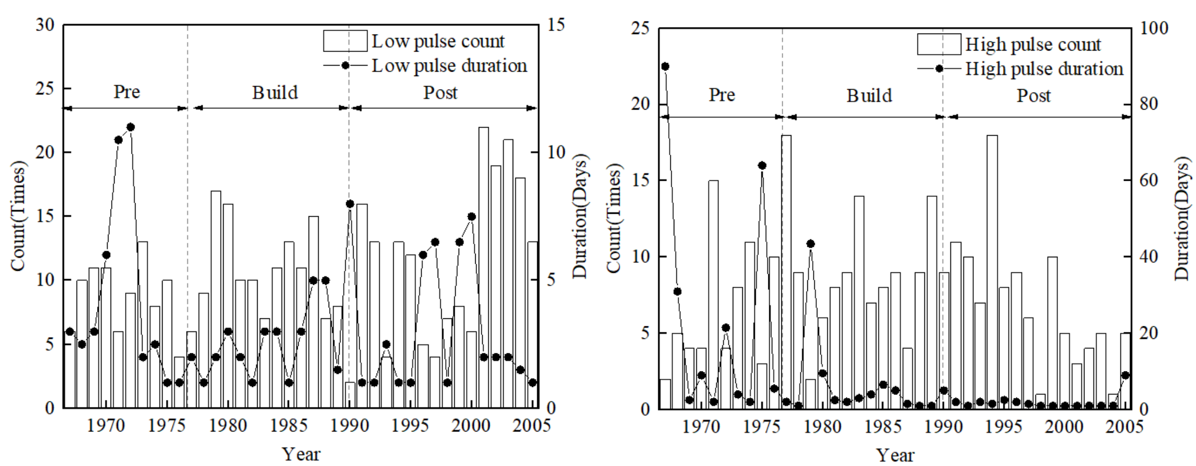


(a) Low pulse (b) High pulse

Figure 12. Count and duration of high and low flow pulses for Lanzhou station

*Analysis of the rate and frequency of water condition changes*

accepted version: https://doi.org/10.1007/s00477-020-01926-6

The frequency alterations of fall rate of Maqu station in both under- and post-construction periods are 0.10. After considering the morphological alteration, the overall alterations of the 5th group IHAs are defined as high (0.69, 0.54 and 0.67) during the under-construction period. In the post-construction period, the overall alterations of rise and fall rates are defined as medium (0.49 and 0.33), while the overall alteration of the number of reversals is defined as high (0.66).

For Lanzhou station, in the under- and post-construction periods, all the median values of the rate and frequency of water condition changes show an increasing tendency (see Figure 13), and the frequency alterations are higher than the morphological alterations (see Table 4). The overall alterations of these three parameters are high or medium level in under- and post-construction periods. A growth in rise rate (or fall rate) would decrease the transition time for water flow from low to high (or from high to low), which gives aquatic organisms less time to seek shelter and makes them vulnerable to being washed away (or stranded) by the high (low) flow.

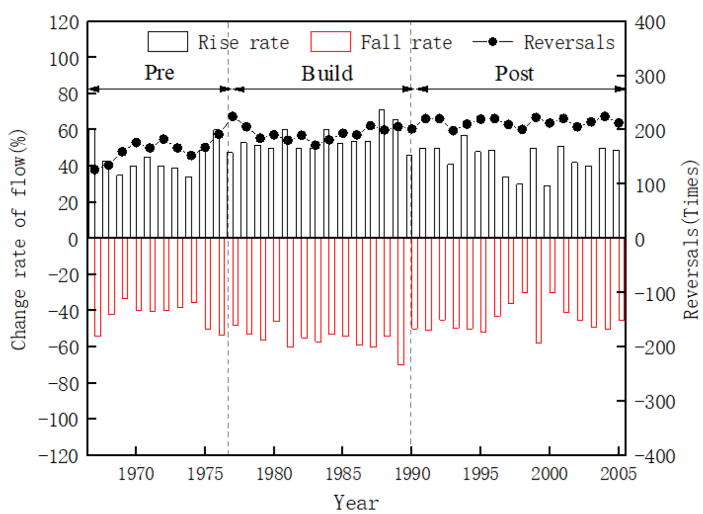


Figure 13. Change rate of flow and number of reversals for Lanzhou station

Total frequency alterations of Maqu in both the under- and post-construction periods are medium level (0.42 and 0.48, respectively). Total morphological alterations of Maqu in the two periods are 0.38 (medium) and 0.25 (low). Thus, the total overall alterations calculated by equations (7) and (8) are 0.63 (high) and 0.60 (medium), respectively. Total frequency alteration of Lanzhou station in the under- and post-construction periods are 0.36 and 0.51 (both are medium level). Total morphological alterations in the two periods are 0.35 and 0.31 (both in medium level). The total overall alterations of Lanzhou are 0.59 (medium) and 0.66 (medium), respectively.

## 4.3 Evaluation of RVA and the new revised method

Several parts of the results show the new method is more reasonable. The first one is the frequency alterations of some IHAs could not match the changes in their median values. In the results of Maqu station (Table 3), although the relative difference of median value of the average monthly flow in July changed 42.99% during under-construction period, the frequency alteration still be 0.08. To verify if the result of traditional RVA is appropriate, the IHA result of this parameter is plotted in Figure 14. It's obvious that the average monthly flow suddenly went up at the beginning of the 1980s. However, the number of IHA values falling into the RVA boundaries in the under-construction period is still 5. Considering the expect year is 5.45 (5*12/11), the result of frequency alteration would be negligible. There is no doubt that the extreme average monthly flow could impact on the local eco-system. Thus, the result of the morphological alteration of this IHA in the same period, which is 0.35, seems more reasonable. Similar proofs can be found in many IHAs, such as the average monthly flow of December, 1-day maximum flow, 3-day maximum flow, etc. For Lanzhou station, compared with the pre-construction period, the median value of high pulse duration decreases by 50.00% and 77.27% in the under-construction and post-construction periods, respectively. Although the median value does change a lot during the latter two periods, high pulse duration exhibits nearly no frequency alteration (0.10) in the under-construction period and medium frequency alteration (0.59) in the post-construction period. The underestimation in the under-construction period is mainly due to that the median value does not move out of the RVA range. Recalling the high pulse duration in Figure 12 (b), most dots are

accepted version: https://doi.org/10.1007/s00477-020-01926-6

distributed near the lower boundary. In this case, a value falling within the statistical range may move out of the statistical range due to a tiny change, which might be another reason for the underestimation or overestimation of traditional RVA. By considering morphological alteration, the overall alteration in the under-construction period changes to 0.29 and the difference between the alteration in the under-construction and post-construction periods is reduced from 0.49 to 0.38.

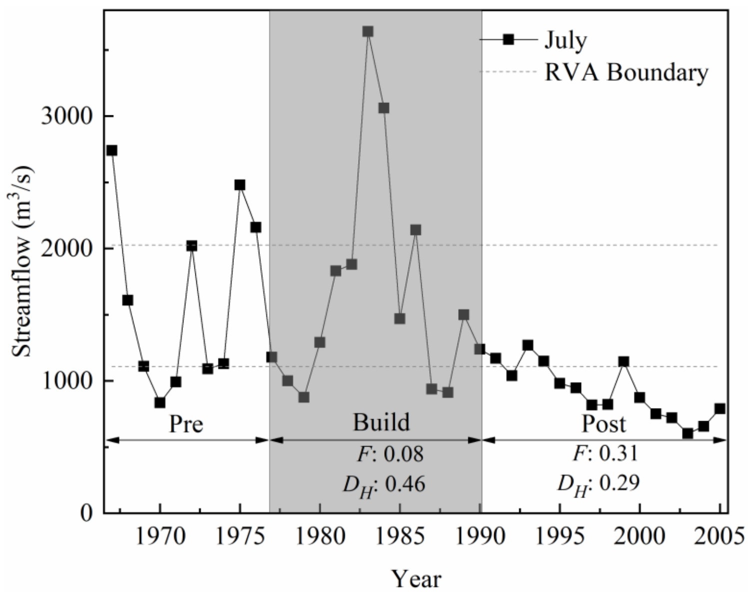


Figure 14. Average monthly flow of July for Maqu station

Another obviously unreasonable results are the average monthly flow of February and the 3-day minimum flow of Lanzhou station. There are nearly no frequency alterations in the average monthly flow of February in the under-construction period and the post-construction period because the number of the years falling in the RVA range has few changes (see Figure 7 (c)). In fact, the average monthly flow of February does change significantly since the dam was built. It begins in the low-value section, dramatically rises to the high-value section during the pre-construction period and shows obvious periodicity in the under-construction period. Subsequently, it slides to the low-value section from the peak and back to the middle-value section in the post-construction period. These changes are well identified by considering the morphological alteration of this IHA parameter. The morphological alterations of the average monthly flow of February in

accepted version: https://doi.org/10.1007/s00477-020-01926-6

the under-construction period and the post-construction period are medium (both 0.40). This leads to medium overall alterations of the average monthly flow of February in both under- and post-construction period (0.57 and 0.46). Indeed, the morphological characteristics of most IHAs have been changed by dam construction. For Lanzhou station, the 3-day minimum flow has the most significant morphological alteration (0.50) of all IHAs in the under-construction period. It, however, shows nearly no frequency alteration (0.10) in the under-construction period, although the value goes up to a peak and turns to decrease after a fluctuation (see Figure 9 (b)).

Besides, 23 of these 32 IHAs in Lanzhou station show higher morphological alterations than those for Maqu station after the dam was built. In particular, the morphological alterations of the maximum flow for different durations of Lanzhou station in the post-construction period are higher than that in the under-construction period and are higher than that of Maqu station. This proves the test in section 4.1. In Figure 15, the frequency and morphological alterations of all 32 IHA are plotted. There is not much difference in the deviation of the frequency alterations between these two stations. However, the deviations of the morphological alterations are quite different. Compared with Maqu station which is mainly influenced by climate change, the morphological alterations of Lanzhou station seem more deviated. Since the impact of climate change should be similar at these two close gauges, the enlarged deviation in morphological alteration at Lanzhou station compared with that at Maqu station which is considered natural should be attributed to human activities such as the dam regulation. This fits the results in section 4.1. Obviously, traditional RVA cannot properly assess this deviation.

As a whole, some unreasonable aspects of traditional RVA can be well handled with the revised RVA. The consideration of morphological alterations is a beneficial supplement to the traditional RVA.

*accepted version: https://doi.org/10.1007/s00477-020-01926-6*

### 4.4 Advantages of the Hasse Matrix

Several methods can depict the morphological difference between two different time series. The most common and simplest method is the Euclidean distance [*Keogh et al.*, 2009; *Zois et al.*, 2000; *Sung et al.*, 2009]. However, Euclidean distance cannot consider the ordering relationships of the time series, which is an essential characteristic in morphological analysis. The revised RVA attempts to solve this problem by the introduction of Hasse matrix.

Here gives an example to show the necessity for considering the ordering relationships of the time series. There are three sets of time series: TS1(1, 1, 1, 1, 1, 1, 1, 1, 1, 1, 1); TS2(2, 3, 2 , 2, 1, 3, 2, 3, 1, 1, 3); TS3(1, 1, 1, 2, 2, 2, 2, 3, 3, 3, 3) (Figure 16). TS2 and TS3 have the same number of 1, 2 and 3 with different ordering relationships. The Euclidean distances $D_E$ are 20 for both TS1&TS2 and TS1&TS3, meaning that the traditional or $D_E$-based RVAs cannot effectively distinguish the difference between TS1&TS2 and TS1&TS3. The Hasse distances $D_H$ of TS1&TS2 and TS1&TS3 are 0.32 and 0.52, respectively. The Hasse distance between TS1 and TS2 is lower than that between TS1 and TS3 because the scatters of TS2 fluctuate around a horizontal line. This can also be proven by comparing the Hasse matrices of the three-time series (Figure 17). The Hasse matrix of TS2 shows a higher-level disorder compared with the Hasse matrix of TS1 and TS3 in both the diagonal and non-diagonal parts. Compared with TS1, more Non-zero elements can be found in the Hasse matrix of TS3 than TS2. Besides, another interesting thing is the Hasse matrix of TS2 shows a higher-level disorder compared with the Hasse matrix of TS1 and TS3 in both the diagonal and non-diagonal parts since TS2 has a higher fluctuation level. This is proof that the Hasse matrix can depict the changing process of data in time series. In this example, the performance of the Euclidean distance and Hasse matrix are compared. Other examples can be found to prove the necessity for considering the ordering

accepted version: https://doi.org/10.1007/s00477-020-01926-6

relationships too. For example, a detailed comparison between cross recurrence plots and correlation coefficient has been conducted by *Wendi et at.* [2019] which shows the unreasonable result without considering ordering relationships.

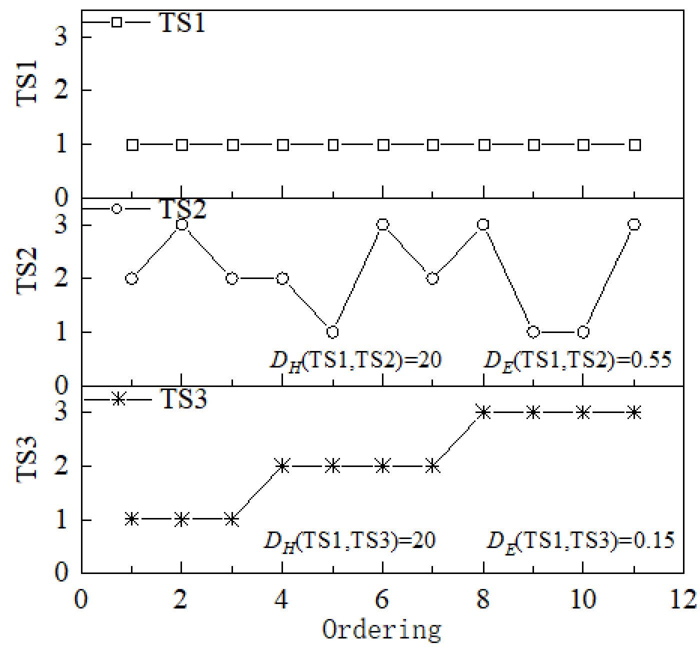


Figure 16. Three time series with different morphological characteristics

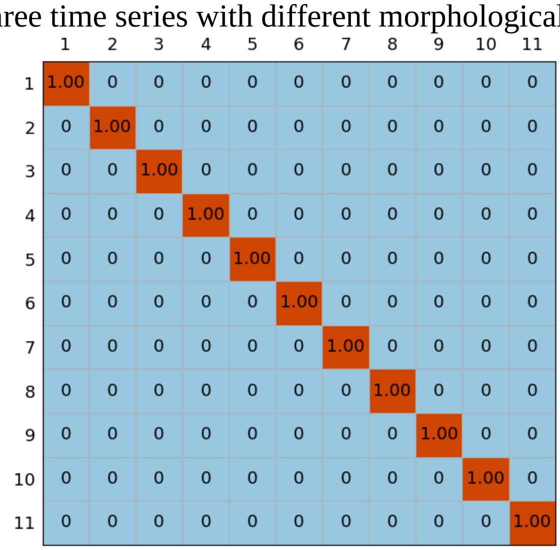


(a) TS1

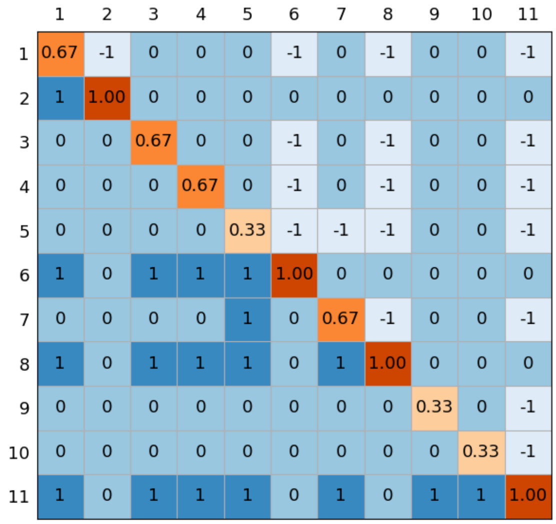


(b) TS2

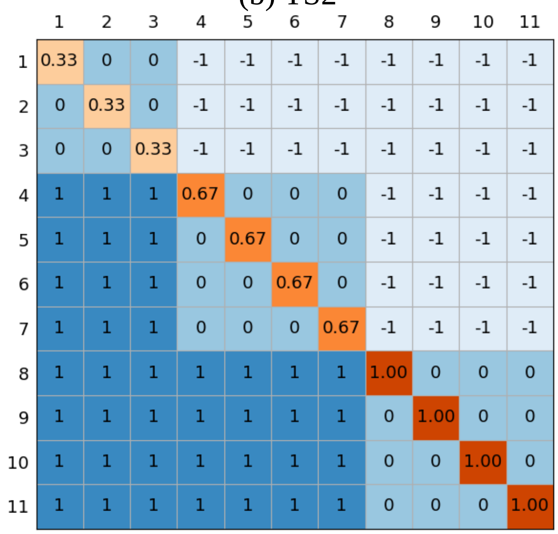


(c) TS3

Figure 17. Hasse Matrices of three sets of time series

In this case study, the most and least significant morphological alterations of Lanzhou station are detected in 3-day minimum flow in the under-construction period (0.50) and fall rate in the post-construction period (0.18), respectively (Table 4). The details of these two parameters are shown in Figure 18. In two time series with the same length (Green and red rectangles), it can be obviously seen that the difference of 3-day minimum flows in two different periods is larger than that of fall rates. The Hasse matrices of 3-day minimum flow in the pre- and under-construction periods are shown in Figure 19 (a) and (b). The Hasse Matrices of fall rate in the pre- and post-construction periods are shown in Figure 19 (c) and (d). It is also easy to see that the difference in

accepted version: https://doi.org/10.1007/s00477-020-01926-6

the number and distribution of Non-zero elements between (a) and (b) is greater than the difference between (c) and (d) in Figure 19.

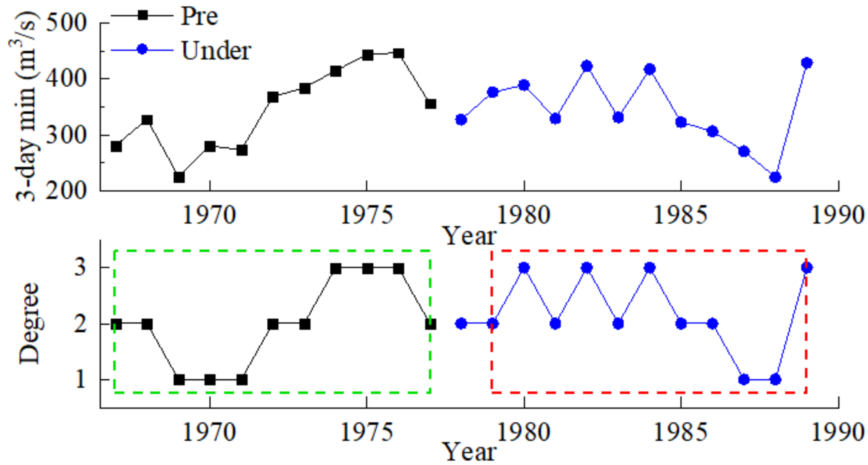


(a) 3-day minimum flow

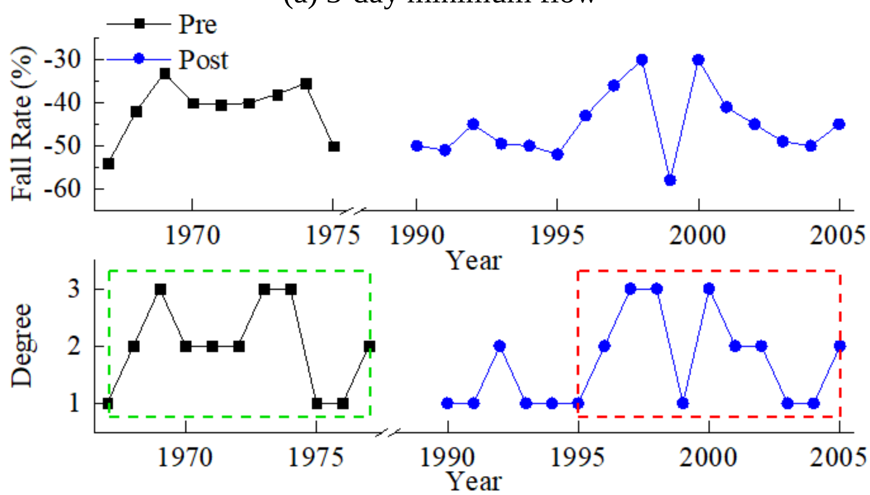


(b) Fall rate

Figure 18. Comparison of 3-day minimum flow (a) and fall rate (b)

*accepted version: https://doi.org/10.1007/s00477-020-01926-6*

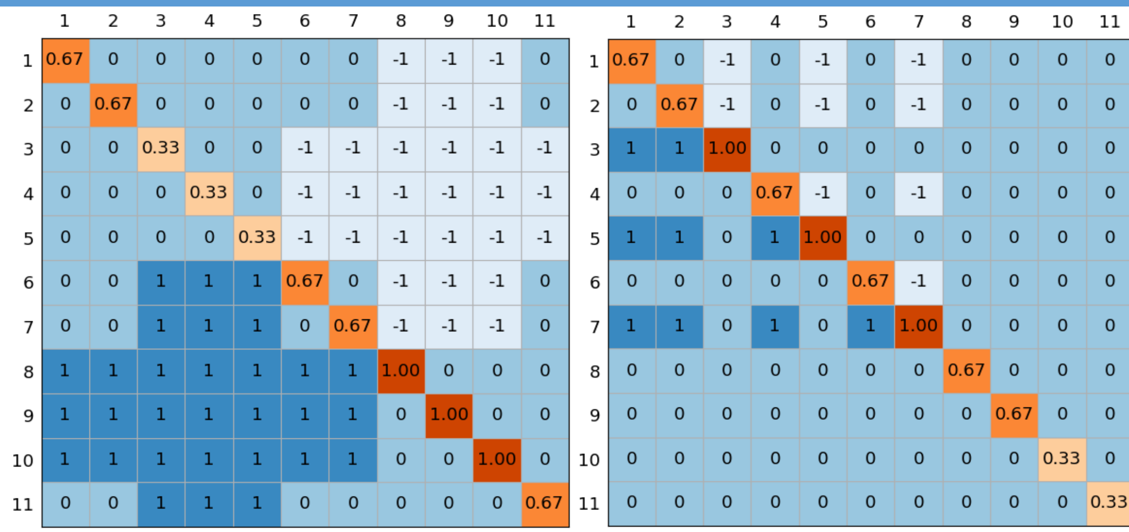


(a) Pre-construction period (3-day min) (b) Under-construction period (3-day min)

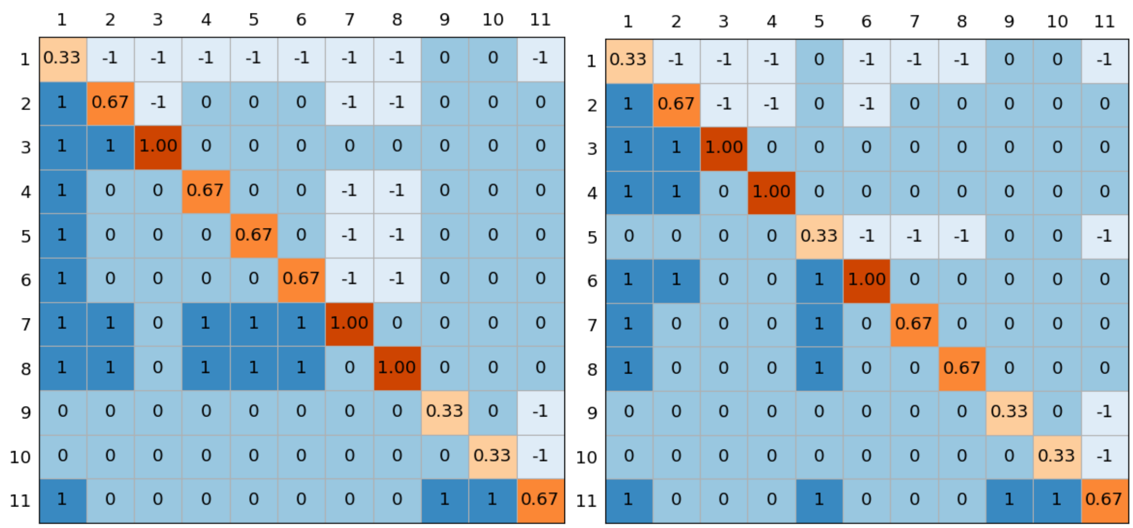


(c) Pre-construction period (fall rate) (d) Under-construction period (fall rate)

Figure 19. Hasse Matrices of 3-day minimum flow (a) (b) and fall rate (c) (d)

## 5 Conclusions

The morphological alteration of IHAs, which is associated to discharge variations in sequence, has a great impact on the river ecosystem, which however cannot be captured by traditional RVA. In this study, we proposed a revised RVA method by considering the morphological alteration of IHAs using Hasse Matrices. The hydrological alterations of two stations in the upper Yellow River are evaluated by both the traditional and revised RVAs. Compared with the traditional RVA, the revised method can offer a more reasonable assessment in the hydrological alteration of flow regime. The main conclusions can be summarized as follows:

(1) Traditional RVA underestimates hydrological alteration because it only considers the frequency alteration of IHAs within the RVA boundaries and it neglects the changes in sequence in consecutive years. The problem can be well solved by considering the morphological alteration of IHAs. To get a complete assessment of the morphological alteration of the time series, it is important to adopt a method that can consider the ordering relationships and magnitude differences of the elements.

(2) The case study of the upper Yellow River shows that the hydrological regime of the upper Yellow River has been changed a lot since 1980s after the construction of Longyangxia dam. The hydrological change may result in the decreasing sand content of the Yellow River and the river is not as fierce as before. Both climate change and human activities extract impacts on the hydrological alterations. However, deviation in alteration in IHAs shows little difference between two gauges with and without dam impact using traditional RVA while apparent differences can be found with revised RVA method, which shows the priority of revised RVA in capturing the flow changes.

(3) The figure of a Hasse matrix is like a fingerprint of a time series. It can reflect how time series changes with time. The changes in the figure represent the morphological alteration degree of a time series. A 2-D feature map of a hydrological time series can be created, based on which future users can try to combine machine learning methods to distinguish the hydrological similarities of different regions through image recognition.

*accepted version: https://doi.org/10.1007/s00477-020-01926-6*

## References

Araújo, R. D. A., Madeiro, F., de Sousa, R. P., Pessoa, L. F. C., & Ferreira, T. A. E. (2006, July). An evolutionary morphological approach for financial time series forecasting. In 2006 IEEE International Conference on Evolutionary Computation (pp. 2467-2474). IEEE, doi: 10.1109/CEC.2006.1688615.

Araújo, R. D. A. (2010). Swarm-based translation-invariant morphological prediction method for financial time series forecasting. Information Sciences, 180(24), 4784-4805, doi: 10.1016/j.ins.2010.08.037.

Bednarek, A. T. (2001). Undamming rivers: a review of the ecological impacts of dam removal. Environmental management, 27(6), 803-814, doi: 10.1007/s002670010189.

Bunn, S. E., & Arthington, A. H. (2002). Basic principles and ecological consequences of altered flow regimes for aquatic biodiversity. Environmental management, 30(4), 492-507, doi: 10.1007/s00267-002-2737-0.

Champely, S., & Chessel, D. (2002). Measuring biological diversity using Euclidean metrics. Environmental and Ecological Statistics, 9(2), 167-177, doi: 10.1023/a:1015170104476.

Chen, Y. D., Yang, T., Xu, C. Y., Zhang, Q., Chen, X., & Hao, Z. C. (2010). Hydrologic alteration along the Middle and Upper East River (Dongjiang) basin, South China: a visually enhanced mining on the results of RVA method. Stochastic Environmental Research and Risk Assessment, 24(1), 9-18, doi: 10.1007/s00477-008-0294-7.

Costigan, K. H., Kennard, M. J., Leigh, C., Sauquet, E., Datry, T., & Boulton, A. J. (2017). Flow regimes in intermittent rivers and ephemeral streams. Intermittent Rivers and Ephemeral Streams, 51-78, doi: 10.1016/B978-0-12-803835-2.00003-6.

Cui, T., Yang, T., Xu, C. Y., Shao, Q., Wang, X., & Li, Z. (2018). Assessment of the impact of climate change on flow regime at multiple temporal scales and potential ecological implications in an alpine river. Stochastic environmental research and risk assessment, 32(6), 1849-1866, doi: 10.1007/s00477-017-1475-z.

Ding, H., Trajcevski, G., Scheuermann, P., Wang, X., & Keogh, E. (2008). Querying and mining of time series data: experimental comparison of representations and distance measures. Proceedings of the VLDB Endowment, 1(2), 1542-1552, doi: 10.14778/1454159.1454226.

Engen, S., Grøtan, V., & Sæther, B. E. (2011). Estimating similarity of communities: a parametric approach to spatio-temporal analysis of species diversity. Ecography, 34(2), 220-231, doi: 10.1111/j.1600-0587.2010.06082.x.

Eum, H. I., Dibike, Y., & Prowse, T. (2017). Climate-induced alteration of hydrologic indicators in the Athabasca River Basin, Alberta, Canada. Journal of hydrology, 544, 327-342, doi: 10.1016/j.jhydrol.2016.11.034.

Feng, J., Wang, T., & Xie, C. (2006). Eco-environmental degradation in the source region of the Yellow River, Northeast Qinghai-Xizang Plateau. Environmental Monitoring and Assessment, 122(1-3), 125-143, doi: 10.1007/s10661-005-9169-2.

Ge, J., Peng, W., Huang, W., Qu, X., & Singh, S. (2018). Quantitative assessment of flow regime alteration using a revised range of variability methods. Water, 10(5), 597, doi: 10.3390/w10050597.

Huang, F., Li, F., Zhang, N., Chen, Q., Qian, B., Guo, L., & Xia, Z. (2017). A histogram comparison approach for assessing hydrologic regime alteration. River research and applications, 33(5), 809-822, doi: 10.1002/rra.3130.

Keogh E, Wei L, Xi X, et al. Supporting exact indexing of arbitrarily rotated shapes and periodic time series under euclidean and warping distance measures[J]. The VLDB journal, 2009, 18(3): 611-630.

Kozlowski, T. T. (2002). Physiological-ecological impacts of flooding on riparian forest ecosystems. Wetlands, 22(3), 550-561, doi: 10.1672/0277-5212(2002)022[0550:peiofo]2.0.co;2.

Lacasa, L., Nicosia, V., & Latora, V. (2015). Network structure of multivariate time series. Scientific reports, 5, 15508, doi: 10.1038/srep15508.

Lin, K., Lin, Y., Liu, P., He, Y., & Tu, X. (2016). Considering the Order and Symmetry to Improve the Traditional RVA for Evaluation of Hydrologic Alteration of River Systems. Water Resources Management, 30(14), 5501-5516, doi: 10.1007/s11269-016-1502-8.

McDaniel, R. D., & O’Donnell, F. C. (2019). Assessment of Hydrologic Alteration Metrics for Detecting Urbanization Impacts. Water, 11(5), 1017, doi: 10.3390/w11051017.

Mendoza-Lera, C., Federlein, L. L., Knie, M., & Mutz, M. (2016). The algal lift: Buoyancy-mediated sediment transport. Water Resources Research, 52(1), 108-118, doi: 10.1002/2015WR017315.

Milbourn, T. T., Boot, A. W., & Thakor, A. V. (1999). Megamergers and expanded scope: Theories of bank size and activity diversity. Journal of Banking & Finance, 23(2-4), 195-214, doi: 10.1016/S0378-4266(98)00079-X.

Oliver, A. A., Dahlgren, R. A., & Deas, M. L. (2014). The upside-down river: Reservoirs, algal blooms, and tributaries affect temporal and spatial patterns in nitrogen and phosphorus in the Klamath River, USA. Journal of Hydrology, 519, 164-176, doi: 10.1016/j.jhydrol.2014.06.025.

Pavan, M., & Todeschini, R. (2004). New indices for analysing partial ranking diagrams. Analytica chimica acta, 515(1), 167-181, doi: 10.1016/j.aca.2003.11.019.

Richter, B. D., Baumgartner, J. V., Powell, J., & Braun, D. P. (1996). A method for assessing hydrologic alteration within ecosystems. Conservation biology, 10(4), 1163-1174, doi: 10.1046/j.1523-1739.1996.10041163.x.

Richter, B., Baumgartner, J., Wigington, R., & Braun, D. (1997). How much water does a river need?. Freshwater biology, 37(1), 231-249, doi: 10.1046/j.1365-2427.1997.00153.x.

Richter, B. D., Baumgartner, J. V., Braun, D. P., & Powell, J. (1998). A spatial assessment of hydrologic alteration within a river network. Regulated Rivers: Research & Management, 14(4), 329-340, doi: 10.1002/(SICI)1099-1646(199807/08)14:43.0.CO;2-E.

Shiau, J. T., & Wu, F. C. (2008). A histogram matching approach for assessment of flow regime alteration: application to environmental flow optimization. River Research and Applications, 24(7), 914-928, doi: 10.1002/rra.1102.

Suen, J. P., & Eheart, J. W. (2006). Reservoir management to balance ecosystem and human needs: Incorporating the paradigm of the ecological flow regime. Water resources research, 42(3) , doi: 10.1029/2005WR004314.

Suen, J. P. (2010). Potential impacts to freshwater ecosystems caused by flow regime alteration under changing climate conditions in Taiwan. Hydrobiologia, 649(1), 115-128, doi: 10.1007/s10750-010-0234-7.

Sung, P., Syed, Z., & Guttag, J. (2009, April). Quantifying morphology changes in time series data with skew. In 2009 IEEE International Conference on Acoustics, Speech and Signal Processing (pp. 477-480). IEEE.

Syed, Z., Scirica, B. M., Stultz, C. M., & Guttag, J. V. (2008, September). Risk-stratification following acute coronary syndromes using a novel electrocardiographic technique to measure variability in morphology. In 2008 Computers in Cardiology (pp. 13-16). IEEE.

Todeschini, R., Ballabio, D., Consonni, V., & Mauri, A. (2007). A new similarity/diversity measure for sequential data. MATCH Commun. Math. Comput. Chem, 57, 51-67, doi: 10.1007/s00229-006-0054-2.

Tonkin, J. D., Merritt, D. M., Olden, J. D., Reynolds, L. V., & Lytle, D. A. (2018). Flow regime alteration degrades ecological networks in riparian ecosystems. Nature ecology & evolution, 2(1), 86, doi: 10.1038/s41559-017-0379-0.

*accepted version: https://doi.org/10.1007/s00477-020-01926-6*

Trinci, G., Harvey, G. L., Henshaw, A. J., Bertoldi, W., & Hölker, F. (2017). Life in turbulent flows: interactions between hydrodynamics and aquatic organisms in rivers. Wiley Interdisciplinary Reviews: Water, 4(3), e1213, doi: 10.1002/wat2.1213.

Wang, Y., Rhoads, B. L., & Wang, D. (2016). Assessment of the flow regime alterations in the middle reach of the Yangtze River associated with dam construction: potential ecological implications. Hydrological processes, 30(21), 3949-3966, doi: 10.1002/hyp.10921.

Wang, X., Yang, T., Wortmann, M., Shi, P., Hattermann, F., Lobanova, A., & Aich, V. (2017). Analysis of multi-dimensional hydrological alterations under climate change for four major river basins in different climate zones. Climatic Change, 141(3), 483-498, doi: 10.1007/s10584-016-1843-6.

Wang, X., Yang, T., Yong, B., Krysanova, V., Shi, P., Li, Z., & Zhou, X. (2018). Impacts of climate change on flow regime and sequential threats to riverine ecosystem in the source region of the Yellow River. Environmental earth sciences, 77(12), 465, doi: 10.1007/s12665-018-7628-7.

Wendi, D., Merz, B., & Marwan, N. (2019). Assessing Hydrograph Similarity and Rare Runoff Dynamics by Cross Recurrence Plots. Water Resources Research, 55(6), 4704-4726.

Woodward, G., Bonada, N., Brown, L. E., Death, R. G., Durance, I., Gray, C., ... & Thompson, R. M. (2016). The effects of climatic fluctuations and extreme events on running water ecosystems. Philosophical Transactions of the Royal Society B: Biological Sciences, 371(1694), 20150274, doi: 10.1098/rstb.2015.0274.

Wu, X., Bi, N., Kanai, Y., Saito, Y., Zhang, Y., Yang, Z., ... & Wang, H. (2015). Sedimentary records off the modern Huanghe (Yellow River) delta and their response to deltaic river channel shifts over the last 200 years. Journal of Asian Earth Sciences, 108, 68-80, doi: 10.1016/j.jseaes.2015.04.028.

Xue, L., Zhang, H., Yang, C., Zhang, L., & Sun, C. (2017). Quantitative assessment of hydrological alteration caused by irrigation projects in the Tarim River basin, China. Scientific reports, 7(1), 4291, doi: 10.1038/s41598-017-04583-y.

Yang, P., Yin, X. A., Yang, Z. F., & Tang, J. (2014). A revised range of variability approach considering the periodicity of hydrological indicators. Hydrological processes, 28(26), 6222-6235, doi: 10.1002/hyp.10106.

Yang, T., Zhang, Q., Chen, Y. D., Tao, X., Xu, C. Y., & Chen, X. (2008). A spatial assessment of hydrologic alteration caused by dam construction in the middle and lower Yellow River, China. Hydrological Processes, 22(18), 3829-3843, doi: 10.1002/hyp.6993.

Yang, T., Xu, C. Y., Shao, Q., Chen, X., Lu, G. H., & Hao, Z. C. (2010). Temporal and spatial patterns of low-flow changes in the Yellow River in the last half century. Stochastic Environmental Research and Risk Assessment, 24(2), 297-309, doi: 10.1007/s00477-009-0318-y.

Yang, T., Cui, T., Xu, C. Y., Ciais, P., & Shi, P. (2017). Development of a new IHA method for impact assessment of climate change on flow regime. Global and planetary change, 156, 68-79, doi: 10.1016/j.gloplacha.2017.07.006.

Yao, W., Xiao, P., Shen, Z., Wang, J., & Jiao, P. (2016). Analysis of the contribution of multiple factors to the recent decrease in discharge and sediment yield in the Yellow River Basin, China. Journal of Geographical Sciences, 26(9), 1289-1304, doi: 10.1007/s11442-016-1227-7.

Yin, X. A., Yang, Z. F., & Petts, G. E. (2015). A new method to assess the flow regime alterations in riverine ecosystems. River research and applications, 31(4), 497-504, doi: 10.1002/rra.2817.

Yu, C., Yin, X. A., & Yang, Z. (2016). A revised range of variability approach for the comprehensive assessment of the alteration of flow regime. Ecological Engineering, 96, 200-207, doi: 10.1016/j.ecoleng.2015.12.001.

Yu, Q., Huang, Q., & Zhang, H. (2010). Influence of different reservoir operations on the eco-hydrological characteristics variability of Lanzhou Gauge of the Yellow River. Arid Land Geography, 33(5), 747-755, doi: 10.1017/S0004972710001772.

Zhang, Z., Huang, Y., & Huang, J. (2016). Hydrologic alteration associated with dam construction in a medium-sized coastal watershed of southeast China. Water, 8(8), 317, doi: 10.3390/w8080317.

Zois, E. N., & Anastassopoulos, V. (2000). Morphological waveform coding for writer identification. Pattern Recognition, 33(3), 385-398.

Zolezzi, G., Bellin, A., Bruno, M. C., Maiolini, B., & Siviglia, A. (2009). Assessing hydrological alterations at multiple temporal scales: Adige River, Italy. Water Resources Research, 45(12), doi: 10.1029/2008WR007266.